processes

MDPI

Review

A Review of Methane Activation Reactions by Halogenation: Catalysis, Mechanism, Kinetics, Modeling, and Reactors

David Bajec, Matic Grom, Damjan Lašič Jurković, Andrii Kostyniuk, Matej Huš, Miha Grilc, Blaž Likozar and Andrej Pohar *

Department of Catalysis and Chemical Reaction Engineering, National Institute of Chemistry, Hajdrihova 19, 1000 Ljubljana, Slovenia; david.bajec@ki.si (D.B.); matic.grom@ki.si (M.G.); damjan.lasic@ki.si (D.L.J.); andrii.kostyniuk@ki.si (A.K.); matej.hus@ki.si (M.H.); miha.grilc@ki.si (M.G.); blaz.likozar@ki.si (B.L.)
* Correspondence: andrej.pohar@ki.si; Tel.: +386-1-4760-285

Received: 10 March 2020; Accepted: 6 April 2020; Published: 9 April 2020

Abstract: Methane is the central component of natural gas, which is globally one of the most abundant feedstocks. Due to its strong C–H bond, methane activation is difficult, and its conversion into value-added chemicals and fuels has therefore been the pot of gold in the industry and academia for many years. Industrially, halogenation of methane is one of the most promising methane conversion routes, which is why this paper presents a comprehensive review of the literature on methane activation by halogenation. Homogeneous gas phase reactions and their pertinent reaction mechanisms and kinetics are presented as well as microkinetic models for methane reaction with chlorine, bromine, and iodine. The catalysts for non-oxidative and oxidative catalytic halogenation were reviewed for their activity and selectivity as well as their catalytic action. The highly reactive products of methane halogenation reactions are often converted to other chemicals in the same process, and these multi-step processes were reviewed in a separate section. Recent advances in the available computational power have made the use of the ab initio calculations (such as density functional theory) routine, allowing for in silico calculations of energy profiles, which include all stable intermediates and the transition states linking them. The available literature on this subject is presented. Lastly, green processes and the production of fuels as well as some unconventional methods for methane activation using ultrasound, plasma, superacids, and light are also reviewed.

Keywords: methane; halogenation; catalysis; density functional theory; kinetics; mechanism

1. Introduction

Methane is the main part of natural gas, biogas, and crystalline hydrates at the continental slopes into oceans. The major part (more than 90%) of natural gas is burned for heating, cooking, transportation, and electricity production, which is not a cost effective pathway. Industrially, methane is converted to syngas by steam reforming, which can then be used to synthesize olefins through the Fischer–Tropsch process [1] or methanol through syngas to methanol processes [2,3]. The obtained methanol can be further converted to olefins [4] or gasoline [5,6] or aromatics [7]. This indirect method of methane valorization is costly and economically viable only on a large scale. Direct conversion of methane into valuable chemicals over heterogeneous catalysts in mild conditions is therefore of great interest for the industry and academic community, but the main difficulty with methane activation stems from its strong C–H bond and that conversion of methane has to be carried out at high temperatures, usually above 1000 K [8]. The two most studied methods of methane conversion over heterogeneous catalysts are oxidative coupling of methane (OCM) [9] and non-oxidative methane

dehydroaromatization (MDA) [10]. Both of these approaches have significant disadvantages. In OCM, oxygen or air is co-fed into the reactor and therefore the yield of C_2 hydrocarbons is reduced by the formation of CO_2 and CO [9]. In the MDA reaction, the main problem is catalyst deactivation because of coking at high temperatures [10]. However, single atom catalysts may be able to overcome this problem in non-oxidative methane conversion to C_2 hydrocarbons and aromatics, as it has been recently demonstrated by Xie et al. [11] who prepared a single atom Pt/CeO_2 catalyst and by Guo et al. [12] with their single atom Fe/SiO_2 catalyst. Typically, direct methane conversion processes have difficulty reaching economic viability due to the low yields of desired products [13], but catalytic methane halogenation is an attractive method for methane valorization, especially chlorination and bromination, because these reactions can be carried out under moderate reaction conditions (1 bar and 800 K), with relatively high yields, and their reaction products are versatile platform molecules that can be converted into higher value-added chemicals and liquid fuels [14]. Moreover, methane halogenation reactions can be conducted in the presence or absence of a catalyst, producing halomethanes. Different zeolite catalysts can be used for the conversion of halomethanes. SAPO-34 zeolite can be used for the coupling of methyl bromide [15] or methyl chloride [16] to olefins. Dibromomethane can also be converted to light olefins or methyl bromide by hydrodebromination over different catalysts [17]. Additionally, it is possible to recover the hydrogen halide that is the inevitable byproduct in the halogenation of methane by means of molten salt chemical looping [18] or oxidation [19]. It is known that only methane chlorination and bromination reactions are interesting for a large scale process [20], because fluorine is too reactive, toxic, and corrosive, while the reaction of methane with iodine is thermodynamically limited, and methyl iodide products easily decompose at high temperatures. Halogenation of methane can be achieved thermally, photochemically, or catalytically. This review focuses on the publications relevant for industrial implementation of the methane halogenation process, covering also mechanistic, kinetic, and available ab initio insights as well as unconventional technologies.

2. Homogeneous Gas Phase Reactions

Gas phase halogenation of methane has been thoroughly investigated in the past. The gas phase homogeneous bromination of methane was studied in 1944 by Kistiakowsky and Van Artsdalen [21]. They studied the mechanism and kinetics of photochemical and thermal bromination of methane in a batch quartz reaction cell in the temperature range of 150–230 °C and at 297 °C, respectively. The mechanisms for photochemical and thermal bromination were essentially the same with the only difference being that the energy to break the bromine molecule into Br radicals was provided by light in the first case and by heat in the second case. More recently it was found that two product distributions are observed in methane bromination, namely a kinetic and a thermodynamic one [22]. When residence time in the plug flow reactor is short the kinetic product distribution is obtained, in which case the selectivity for methyl bromide is low. If the residence time is increased from 10 s to 45 s, the products undergo reproportionation, and the selectivity for methyl bromide becomes higher. The selectivity for methyl bromide at 500 °C and 10 s was 50% while at 45 s at the same temperature it was about 70%. This observation is different from methane chlorination where only the kinetic product distribution is observed and from methane iodation where only the thermodynamic product distribution is observed [22]. Gas phase chlorination of methane in a flow reactor equipped with jets for introducing chlorine along the reactor was investigated for industrial use in 1942 [23]. The high velocity of chlorine introduced through jets prevents burning of the mixture due to the exothermic nature of chlorination reactions. The temperature of the reacting gas mixture is thus kept below 500 °C and coke formation is also suppressed. It was found that the Cl_2/CH_4 ratio has a great influence on the product distribution. As expected, selectivity approaches 100% for CCl_4 when the ratio approaches the value of 4. Vice versa, by decreasing the ratio, the product distribution shifts towards CH_3Cl, and as the ratio approaches zero the selectivity for CH_3Cl approaches 100% as is typical for consecutive reactions.

Much later in 1965, the gas-phase iodine reaction was studied by Golden et al. [24] and equilibrium constants for the reaction were measured.

The first kinetic study of thermal chlorination of methane was made in 1931 by Pease and Walz [25] (while Dumas reported the oldest method of halogenation by substitution of alkanes in 1840 [26]). They noted that methane and chlorine react at 400 °C, and conducted experiments at the safer temperature of 250 °C. The products included methyl chloride, methylene dichloride, chloroform, and carbon tetrachloride, with equivalent amounts of HCl, if methane is in excess. If chlorine is in excess, the mixtures are explosive, and carbon and hydrogen chloride are the main products. They also found that oxygen had a powerful inhibitory action. The following reactions were determined to take place [25]:

$$CH_4 + Cl_2 \rightarrow CH_3Cl + HCl \quad (1)$$

$$CH_3Cl + Cl_2 \rightarrow CH_2Cl_2 + HCl \quad (2)$$

$$CH_2Cl_2 + Cl_2 \rightarrow CCl_4 + HCl \quad (3)$$

$$CHCl_3 + Cl_2 \rightarrow CCl_4 + HCl \quad (4)$$

The kinetics followed a second order reaction at atmospheric pressure, with the activation energy of 132.3 kJ/mol:

$$-\frac{d[Cl_2]}{dt} = k_1[CH_4][Cl_2] \quad (5)$$

Aglulin et al. [27] found similar kinetic orders. Adding oxygen showed a considerable decrease in the reaction rate. The inhibitory effect was proportional to the concentration and independent of methane concentration:

$$-\frac{d[Cl_2]}{dt} = k_2\frac{[Cl_2]^2}{[O_2]} \quad (6)$$

It was assumed that oxygen terminates the chain of reaction.

In 1942, McBee et al. [23] published a paper on the chlorination of methane by application of the Hass–McBee chlorination technique. With this technique, a hydrocarbon flows through the reactor and jets of chlorine are positioned at suitable locations. This prevents an explosive or burning reaction by reducing the local chlorine concentrations, which are kept below the explosive mixture limit, since the chlorination reaction is highly exothermic. They found that appropriate stoichiometry ratios between methane and chlorine produce the desired chloromethane. They conducted experiments at 440 °C and determined the same reactions take place as previously reported by Pease and Walz [25]. They found that they could obtain any desired ratio of chloromethanes, and carbon tetrachloride could be obtained in a single pass without recycling.

Pritchard et al. [28] studied several gas phase reactions of chlorine atoms, including methane at 0–300 °C. They found that the overall reaction rates are very sensitive to impurities, to the condition of the surface of the reaction vessel, and to the intensity of the absorbed light, which makes it difficult to determine the rate constants. Around the same time, Krstiakowsky and Artsdales [21] studied photochemical methane bromination. They found that the reactions take place according to the following chain mechanism [21]:

$$Br_2 + (h\nu \text{ or heat}) \rightarrow Br + Br \quad (7)$$

$$Br + CH_4 \rightarrow CH_3 + HBr \quad (8)$$

$$CH_3 + Br_2 \rightarrow CH_3Br + Br \quad (9)$$

$$CH_3 + HBR \rightarrow CH_4 + Br \quad (10)$$

$$Br + Br + M \rightarrow Br_2 + M \quad (11)$$

Hydrogen bromide inhibits bromination of methane. The same mechanism applies if thermal bromination is applied instead of photochemical bromination; 570 °C was the reaction temperature, only instead of photochemically, bromine atoms are produced thermally. The activation energy of photochemical methane bromination was determined: 17.8 kcal/mol. They also found the strength of the C–H bond to be 102 kcal/mol at room temperature.

It was determined that the rate of methane photobromination is proportional to the methane concentration, to the square root of the bromine concentration, and inversely proportional to the square root of the total pressure [21]. The following kinetic expression was obtained for photobromination, where P is the total pressure:

$$-\frac{d[Br_2]}{dt} = \frac{k_3[CH_4][Br_2]^{1/2}[1/P]^{1/2}}{1+\frac{k_4[HBr]}{k_3[Br_2]}} \quad (12)$$

In the second step of the overall photochemical bromination, bromination of methyl chloride takes place:

$$-\frac{d[Br_2]}{dt} = k_4[CH_3Br][Br_2]^{1/2}[1/P]^{1/2} \quad (13)$$

Their bromine equilibrium constant was calculated from the thermodynamic data of Gordon and Barnes [29,30]. These rate expressions were also applied by Degirmenci et al. [30] in a methane halogenation study. Their thermodynamic analysis revealed that bromine was the most suitable halogen. They also found that the conversion of methane and the selectivity of CH_2Br_2 decrease if the amount of bromine in the feed was decreased.

Arai et al. [31] prepared an extensive study of gas phase thermal chlorination with first order rate equations with respect to chlorine and methane. Some differences between their results and the results of Rozanov and Treger [32] triggered a study by the latter who obtained considerable experimental data for laboratory, pilot plant, and industrial conditions. They studied thermal chlorination of methane and its kinetics in the gas-phase. Their work showed that the form of the rate equation depends on the mode of chain termination and have presented rate equations for the chlorination of methane, methyl chloride, methylene chloride, and chloroform with cross and quadratic law chain terminations. A 1.5 kinetic order with respect to reactants was found.

The following elementary steps were considered [32]:

Chain initiation

$$Cl_2 \rightarrow Cl^\bullet + Cl^\bullet \quad (14)$$

Chain propagation

$$Cl^\bullet + RH \rightarrow HCl + R^\bullet \quad (15)$$

$$R^\bullet + Cl_2 \rightarrow RCl + Cl^\bullet \quad (16)$$

Chain termination

$$Cl^\bullet + Cl^\bullet + M \rightarrow Cl_2 + M \quad (17)$$

$$R^\bullet + R^\bullet \rightarrow R\text{-}R \quad (18)$$

$$R^\bullet + Cl^\bullet \rightarrow RCl \quad (19)$$

$$Cl^\bullet + \text{wall} \rightarrow Cl_{ads} \quad (20)$$

The cleavage of the halogen bond to separate chlorine atoms is initiated by the heat. The atoms produced are free radicals. In the second step, a halogen radical reacts with methane to form HCl and a methyl free radical. The methyl free radical then reacts with another chlorine molecule forming methyl chloride and a free chloride radical, by which the process can continue [26]. The reactions are exothermic and high temperature will favor multiple chlorinated products. The free-radical chain mechanism is terminated by the production Cl_2 and methyl chloride, which do not continue the cycle.

A more complex 21-step chlorination reaction scheme with 152 reactions and 38 species was put forward by Tirtowidjo [33] at the AIChE (American Institute of Chemical Engineers) Annual Meeting in 1997. The reaction mechanism is presented in Table S1 in the Supplementary Materials with the Arrhenius constants. These reactions were modeled with computational fluid dynamics (CFD) simulations by Shah and Fox [34] and Raman et al. [35], who used an adiabatic, jet-stirred chlorination reactor for the simulations. CFD allows for studying the transport phenomena together with the underlying complex chemical kinetics and turbulent reacting flows. Shah and Fox [34] found that the product distribution is dependent on the extent of conversion. Methyl chloride was used and chloroform was the desired product in the gas-phase chlorination reactions. It was acknowledged that due to the free radical reactions several by-products can be obtained, which are difficult to separate and the maximum yield of the desirable products occurs around 450 °C.

Upham et al. [36] investigated methane halogenation using iodine and bromine in the gas phase. They also constructed a microkinetic model with rate constants compiled by the National Institute of Science and Technology (NIST) and some were calculated from experimental data. Their elementary steps and Arrhenius constants are presented in Table S2 in the Supplementary Materials. The synthesis of ^{11}C iodomethane as a starting material for production of positron emission spectroscopy tracers was accomplished by gas-phase iodination of ^{11}C methane by P. Larsen et al. [37]. Kinetics of gas-phase reactions between methane and iodine were less studied compared to chlorination and bromination of methane. The kinetics and equilibrium constants of the methane reaction with iodine in the gas-phase were studied in a similar manner by Golden et al. [24] in 1965. The values of equilibrium constants for the reaction of methane with I_2 were determined experimentally at three different temperatures. The values were 1.45×10^{-4}, 2.32×10^{-4}, 4.48×10^{-4}, at 332.4 °C, 357.3 °C, and 393.7 °C, respectively.

3. Catalytic Halogenation

3.1. Non-Oxidative Catalytic Halogenation

Different acidic catalysts for methane bromination and chlorination were prepared by G. A. Olah et al. [38] in the 1980s to increase the selectivity for monohalogenated products above 90%. Gorin et al. [39] studied methane chlorination kinetics in reactions between methane and molten salt consisting of KCl–CuCl–$CuCl_2$ in 1948. This area of research is still active today [40,41]. The highest selectivity achieved for CH_3Br was 99% and 20% conversion of methane over 20% $SbOF_3/Al_2O_3$ at 200 °C, at GHSV (gas hour space velocity) of 100 mL/(g h) and CH_4/Br_2 ratio of 5. The bromine molecule dissociates on the catalyst and the polarized bromine atom acts as an electrophilic reagent to undergo the electrophilic insertion reaction with methane [38]. More recently sulfated zirconia in SBA-15 mesoporous silica was found to also be a selective catalyst for methyl bromide at higher methane conversion. The catalyst is acidic and the mechanism is the same as in the case of the previously mentioned catalyst. At 340 °C the conversion of methane over SZr(25)SBA-15 catalyst was 69% and CH_3B_r selectivity was 99% at GHSV of 3 L/(g h) and 10 Br_2/CH_4 ratio. This is a significant improvement in the CH_3Br yield and provides a promising alternative to other methane activation processes [42]. The acidity of the catalyst is essential for selective methane bromination to methyl bromide. Zeolites are widely known catalysts with a defined pore structure and high surface area. Their acidity varies according to the silica to alumina ratio. Acidic zeolites with low SiO_2/Al_2O_3 could be appropriate catalysts for selective methane bromination. Recently, a broad range of zeolite and zeolite-supported catalysts was screened for bromination and chlorination of methane [40]. It was found that zeolite catalysts are more active in the case of chlorination than in the case of bromination. ZSM-5 and beta zeolites were more than 5 times more active compared to the gas-phase chlorination at 250 °C, 267 h^{-1} GHSV, and CH_4/Cl_2 of 2.43, however the selectivity was rather poor. It was found that the acidic character of zeolites did not play a major role in this study. Altering the SiO_2/Al_2O_3 ratio had almost no effect on the catalytic activity. Similarly, different counter cations and the presence or absence of extra framework aluminum species did not significantly affect the catalytic activity. These findings

suggested that the activity is governed by the production of halogen radicals from homolytic cleavage of the halogen bond on the catalyst surface. This is mainly observed in the chlorination reaction, while in the case of bromination the production of Br radicals has a limited effect on the reaction. In the case of methane chlorination, there is also an additional effect of shape selectivity of zeolite pores, where the sum of kinetic diameters of methane and chlorine radicals is approximately the same as the pore size in some zeolites (e.g., HZSM-5 and beta) [40]. These observations therefore suggest a totally different mechanism of activation on zeolites compared to previously mentioned catalysts, i.e., $SbOF_3/Al_2O_3$ and SZr(25)SBA-15, although strong Brønsted acid sites are present in the zeolites with a low SiO_2/Al_2O_3 ratio.

Similarly as in the case of catalytic bromination of methane, catalytic chlorination of methane was studied by G. A. Olah and I. Busci [43]. They compared performance of amorphous silica-alumina, silicalite, H-mordenite, X, Y, NaL, and H-ZSM-5 zeolite catalysts and found that some zeolites and some other solid acid catalysts improve the selectivity towards monochlorinated methane. Zeolite catalyzed chlorination gave a higher conversion of methane at the temperature range of 200–250 °C compared to the gas-phase reaction alone. In gas phase chlorination, at temperatures below 300 °C, less than 5% conversion of methane was achieved. However, in this temperature range, zeolites were not selective. The selectivity for methyl chloride was substantially improved at temperatures above 300 °C. The best selectivity (99.2%) at 350 °C was achieved with mordenite zeolite. The conversion of methane was 19.1% at GHSV of 600 mL/(g h). The feed CH_4/Cl_2 ratio of 4 was used for the feed mixture. After a few hours of time-on-stream the selectivity for methyl chloride began to drop. This was attributed to the dealumination of the zeolites by HCl since $AlCl_3$ was observed at the outlet of the reactor. The improved selectivity at higher temperature indicated that the mechanism of the reaction over zeolites changes from radical chlorination at lower temperature to the ionic one. It was also pointed out that there is a connection between the acidic properties of zeolites and their selectivity for monochlorination. Zeolites with higher acidity were more active for monochlorination at lower temperatures than zeolites with lower acidity. It was suggested that first chlorine reacts with Brønsted acid to form Al^-OCl^+Si species on the surface of the zeolite. The methane molecule can react with the Cl^+ ion or with the transitional state from Brønsted acid site to Al^-OCl^+Si species. This mechanism is in contrast with the one proposed by a more recent study [40] where the radical mechanism was also assumed for zeolite catalysts. It was also shown that at a lower CH_4/Cl_2 ratio, the zeolite NaHY is less selective for methyl chloride than at a higher ratio [43]. This observation is in agreement with [40], where a CH_4/Cl_2 ratio of 2.43 was used and zeolites were not very selective for methyl chloride. Higher selectivity was achieved at lower conversions of methane. Zeolite Y and zeolite Y supported Pt catalysts (HY, Pt/HY, and Pt/NaY) were studied for selective chlorination of methane by Joo et al. [44] in a fixed-bed continuous flow reactor. In the range of conditions used in their study there was no effect of zeolite Y acidity (when Si/Al ratio of zeolite was varied). The temperature range was 300–350 °C and GHSV was 3 L/(g h). The CH_4/Cl_2 ratio was 1.5. Over Y zeolite, a decrease in CH_3Cl selectivity was observed. The thermal chlorination of methane was still the prevailing reaction pathway with HY catalysts with different acidity. When Pt/HY was used, the conversion of methane increased, but the selectivity to CH_3Cl decreased even more to 60% compared to 64% over HY and to 73.4% selectivity in the case of gas phase chlorination at 350 °C. The increase in conversion was attributed to dissociation of Cl_2 molecules on the Pt particles. With increased abundance of $Cl^\bullet$ radicals, the selectivity for methyl chloride was even lower. A slightly improved yield of methyl chloride was obtained using the Pt/NaY catalyst, which possesses frustrated Lewis pairs, which are useful for ionic cleavage of H_2 to H^+ and H^-. The conversion of CH_4 at 350 °C was around 35% and the selectivity was 60.1%. The authors also observed a spontaneous reaction of methane chlorination without the catalysts at the reaction temperatures above 300 °C.

In another recent study, zeolite Y and MFI zeolites with different Si/Al ratios were compared regarding methyl chloride selectivity in methane chlorination reactions [45]. It was found that the yield of CH_3Cl is generally higher over HY zeolites than over HZSM-5 (MFI structure) zeolites in the range of

experimental conditions used. The reactor temperature was 350 °C, GHSV was 2400 mL/(g h), and the $CH_4/Cl_2/N_2$ ratio was 1/1/5. The best selectivity was achieved using the HY(15) catalyst, namely 49.4% and the conversion was 37.9%. The number in parenthesis is the Si/Al ratio. However, the best yield of methyl chloride was obtained using HY(2.5), the zeolite with the highest acidity. The yield was 19.2%. Compared to the thermodynamic selectivity of methyl chloride (~39%) the catalyzed selectivity was higher (~50%). The effect of the acidity of the catalyst was correlated with methyl chloride yield for Y zeolites, where more acidic zeolites exhibited a higher yield. There was no such correlation for HZSM-5 zeolite, where one maximum yield was achieved with the Si/Al ratio of 40, and the two other tested HZSM-5 zeolites with Si/Al ratios of 15 and 140 exhibited a lower yield of methyl chloride. Therefore it was concluded that not only the acidity, but also the morphology of zeolites affects the yield of methyl chloride. Also the effect of CH_4/Cl_2 ratio was observed, where at a higher ratio the conversion of methane decreased, but the selectivity to methyl chloride increased. At a $CH_4/Cl_2/N_2$ ratio of 2/1/2 the conversion of methane over HY zeolites decreased to 22.1–23.8% and the selectivity increased to 62.5–72.5%, resulting in a lowering of the yield of methyl chloride down to 13.8–16.1%. After the catalytic tests the catalysts were analyzed by XRD (X-ray powder diffraction) and MAS ^{27}Al NMR (magic angle spinning nuclear magnetic resonance). The results confirmed that dealumination took place during the reaction. The catalysts with more aluminum content suffered from framework collapse as a consequence of dealumination caused by HCl. Extra-framework aluminum on the spent catalysts was observed by NMR, further supporting the dealumination. However, catalysts did not deactivate and their catalytic activity remained stable for approximately 380 min of time-on-stream. The overall Al content in the catalyst was also unchanged after the reaction and therefore all the Al species remained on the catalysts. One of the possible forms of Al is $AlCl_3$. The dealumination and redistribution of Al in HZSM-5 when in contact with halogens and hydrogen halides was investigated by V. Paunović et al. [46]. A variety of different characterization techniques were used to investigate the influence on acidity, crystallinity, porosity, and aluminum distribution in ZSM-5 zeolite upon contacting with Br_2, Cl_2, HBr, and HCl at 300–450 °C for 5 h at 1440 mL/(g h). It was found that dealumination of ZSM-5 is more severe when in contact with hydrogen halides than when in contact with Br_2 or Cl_2. A higher degree of dealumination was observed at higher temperatures. HCl acts more strongly than HBr. Halogen in the spent zeolite is coordinated with extra-framework aluminum. It was also shown that ZSM-5 samples, that were in contact with hydrogen halides and halogens at temperatures up to 400 °C can be regenerated by calcination in air at 550 °C for 5 h. The mechanism of hydrogen halides and halogens interaction with ZSM-5 and the mechanism of oxidative regeneration were also proposed based on experimental evidence. Although dealumination took place, the crystalline structure remained intact. This also explains the lack of change in activity during the reaction in the work by Kwon et al. [45], although dealumination took place.

Methane and bromine or chlorine can be converted directly to olefins and hydrogen halide over zeolite catalyst SAPO-34. Batamack et al. [47] showed that when the residence time over SAPO-34 catalyst is long enough, hydrocarbons in the range C_2–C_6 are formed directly. When a methane and bromine mixture was fed into the reactor loaded with SAPO-34 at 365 °C and at a residence time larger than 83 s, the products were methyl bromide, hydrocarbons, and hydrogen bromide. But, when the residence time was smaller than 25 s, the catalyst was selective for methyl bromide and hydrogen bromide. At 365 °C, GHSV of 43.2 mL/(g h), and a CH_4/Br_2 ratio of 10.3, the conversion of bromine was 61.8% and the selectivity for methyl bromide was 36.4%. The rest were hydrocarbons. The majority of hydrocarbon products represented propane, propylene, and ethylene. It is known that methyl bromide can be coupled to light olefins over SAPO-34 [15]. Therefore, if the residence time is large enough, methyl bromide that forms from methane bromination can further couple to olefins [47].

The activity of non-zeolite catalysts has also been reported. CO and CH_4 chlorination were carried out using the onion-like graphene carbon by G. Centi and coauthors [48]. It was shown that the nano-ordering of the hemi-fullerene-type graphene achieved high performance in the selective chlorination due to the decreasing defects, transformation of C–C bonds and as a result irreversible

chemisorption of Cl_2 on catalytic sites. Selective methane bromination into monobromomethane was investigated using sulfated zirconia in the SBA-15 catalyst at 340 °C by V. Degirmenci et al. [42]. The 99% selectivity to CH_3Br with 69% methane conversion at 340 °C was achieved with 25 mol% ZrO_2/SBA-15 catalyst.

Very recently, Paunović et al. [40] studied the catalytic halogenation of methane with a large library of various materials such as: carriers (quartz, SiO_2, SiC, α-Al_2O_3, γ-Al_2O_3 and carbon), noble metals (Pt, Pd and Ru), metal oxides (Fe_2O_3 and CeO_2), chlorides ($PdCl_2$ and $CuCl_2$), and oxyfluorides ($TaOF_3$) supported on SiO_2, γ-Al_2O_3, carbon, or H-ZSM-5 carriers, sulfated systems (S-ZrO_2, S-ZrO_2-SBA-15, S-TiO_2, S-Nb_2O_5, S-Ta_2O_5, and Nafion) and zeolites (3A, H-USY, H-MOR, H-SAPO-34, H-BETA, and H-ZSM-5). The authors found that methane conversion using SiO_2, SiC, α-Al_2O_3, and γ-Al_2O_3 supports are similar to or higher than that of the empty reactor. Mesoporous supports such as SiO_2, and γ-Al_2O_3 showed a higher conversion of methane in comparison to the nonporous quartz, SiC, and α-Al_2O_3, pointing out the positive effect of the surface area on methane halogenation. It was observed that carbon support provided 1.5–2.0 times higher CH_4 conversion than SiO_2 and γ-Al_2O_3, while the product selectivity was similar to quartz support and to the reactor without any catalyst. Pt/carbon, $CuCl_2/SiO_2$, and Fe_2O_3/SiO_2 catalysts exhibited higher chlorination than other supported metal-based catalysts. At the same time, $PdCl_2/SiO_2$ and Fe_2O_3/SiO_2 catalysts displayed the highest selectivity towards CH_3Cl. Over Pt/carbon and $TaOF_3/Al_2O_3$ catalysts, some CO_x products were also forming. When sulfated catalysts were studied, the conversion of CH_4 and Cl_2 were comparable to SiO_2 and γ-Al_2O_3, while the selectivity to CH_3Cl was similar to the empty reactor.

The highest conversion of methane and Cl_2 amongst all studied sulfated catalysts was achieved by the S-TiO_2 catalyst. When the methane chlorination reaction was carried out by zeolite catalysts the highest performance was observed. It was shown that H-BETA-15 and H-ZSM-5-40 had 5.5 times higher activity than the empty reactor and the benchmark quartz reactor, while 3A, H-USY-6, H-MOR-15, and H-SAPO-34 zeolites had similar activity to those of SiO_2 and γ-Al_2O_3 supports. In addition, all studied zeolite catalysts exhibited increased CH_2Cl_2 and $CHCl_3$ fractions. At the same time, all these studied zeolites (excluding H-ZSM-5-40) produced small amounts of CO_x.

Figure 1 shows the performance of various catalysts in the reaction of methane bromination. It was found that CH_4 and Br_2 conversion is 2 times higher using the porous SiO_2 support in comparison to quartz and comparable to the empty reactor, but the product distribution is the same in the low temperature regime. The supported metal-based (except Pt/SiO_2, sector b) and sulfated oxides (except S-ZrO_2-SBA-15, sector c) catalysts had a comparable conversion to the empty reactor and inorganic carriers, while selectivity towards CH_3Br was lower and an additional CO_x generation was observed. When sulfated oxide catalysts were tested, the SO_2 fraction was identified due to their limited stability in a bromination environment. In addition, it was found that zeolite catalysts had in 1–2% higher CH_4 conversion but the product distribution was negatively affected by the coke and CO_x fraction formation.

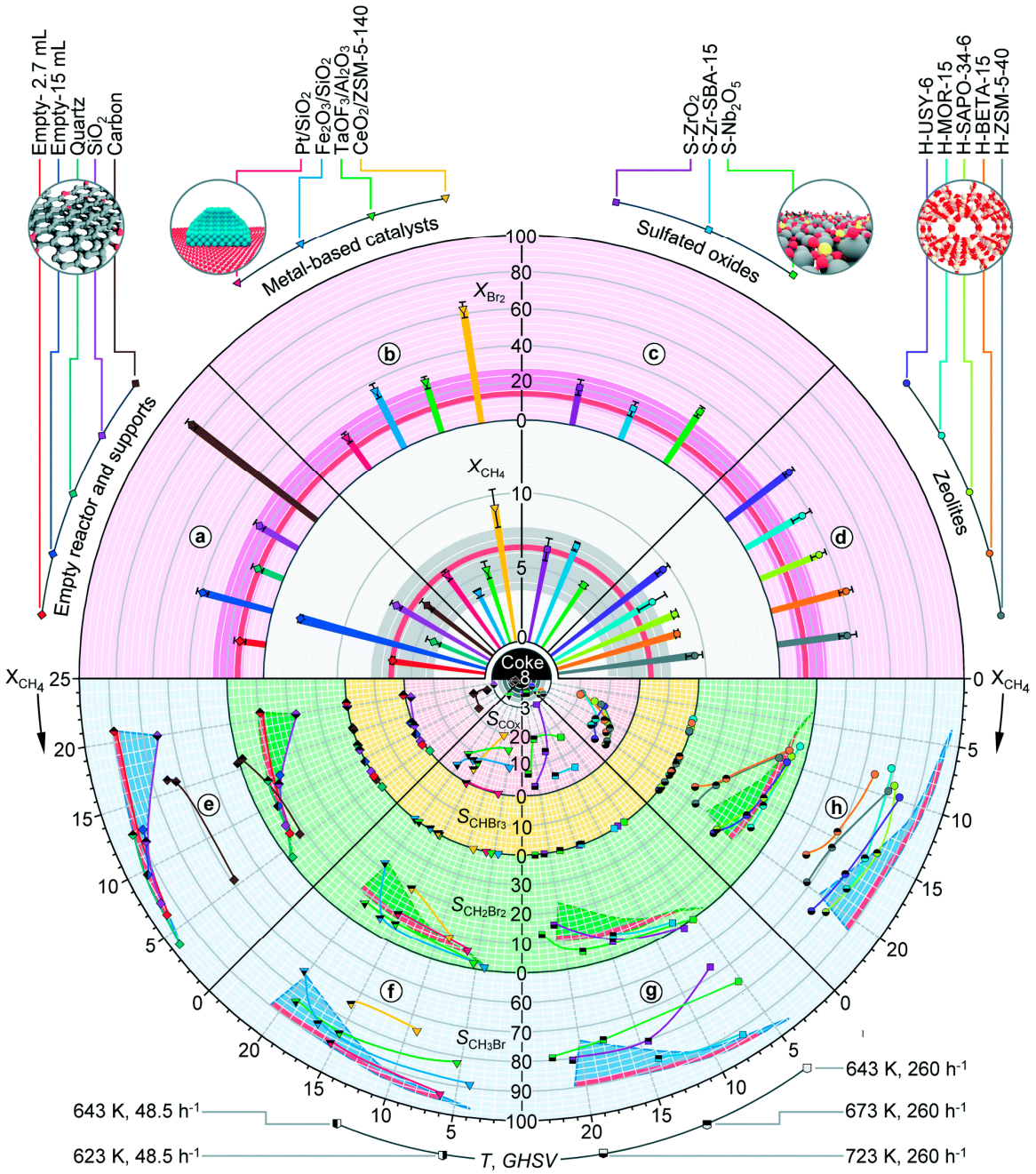

Figure 1. Methane bromination reactions at T = 643 K and GHSV (gas hourly space velocity) = 260 h^{-1} (**a**) in empty reactors and over supports, (**b**) supported metal-based catalysts, (**c**) sulfated oxides, and (**d**) zeolites. Selectivity to different products in methane bromination (**e**) in empty reactors and over supports, (**f**) supported metal-based catalysts, (**g**) sulfated oxides, and (**h**) zeolites as a function of methane conversion, which was adjusted by varying the temperature or GHSV. Conversions and selectivities are expressed in %. Other conditions: CH_4/Br_2 = 8.5/3.2 ± 0.1 and P = 100 kPa. Reprinted from [40], with the permission of the Royal Society of Chemistry, copyright 2019.

The conversion of reactants in methane chlorination over ZSM-5 and BETA zeolite catalysts with different Si/Al ratios, counter ions, mesoporosities, and crystallite sizes at various feed compositions was also studied [40]. The authors declared that the H-ZSM-5-40 is the most active zeolite catalyst in CH_4 chlorination comparing to the empty reactor and various inorganic carriers. The different cations such as Li, Na, Cs, Ca, Fe, Pt, Mg, and Sn were introduced to the ZSM-5-25, H-ZSM-5-140, and H-BETA-220 zeolite frameworks and no effect on the catalytic activity and selectivity was observed.

Only the Li-ZSM-5-25 and Na-ZSM-5-25 catalysts exhibited a higher CH_4 and Cl_2 conversion comparing to the H-ZSM-5-40 and H-ZSM-5-25 pristine zeolites. This catalytic activity of the Li-ZSM-5-25 and Na-ZSM-5-25 catalysts was explained by the appearance of the strong Lewis acid sites, which are important for the chlorination of aromatic compounds. At the same time, the selectivity-conversion results of the Li- and Na-ZSM-5-25 promoted catalysts did not have a significant difference from the others studied parent H-ZSM-5 catalysts.

Based on the literature data we can conclude that the most industrially-relevant and highly active catalysts for methane chlorination via the radical-chain mechanism are H-ZSM-5 and H-BETA zeolites. Their catalytic activity can be explained by the confinement of the radical intermediates and/or transition states and by the impact of the micropore size, intracrystalline mesoporosity, and crystallite size on the product distribution. At the same time, the Si/Al ratios, counter cation, and the formation of the aluminum extra framework did not have a significant effect on the catalytic activity and selectivity in the reaction of CH_4 chlorination over the most active pristine H-ZSM-5 catalysts. Finally, most of the studied catalysts had a limited influence on the methane bromination in comparison to that with non-catalyzed reactions.

3.2. Oxidative Catalytic Halogenation

Catalyst design for oxyhalogenation of methane and catalyst structure–performance relationships were also investigated by Paunović et al. [49–51]. It was pointed out that the catalyst for oxybromination should be able to oxidize HBr on the surface, but at the same time it should not activate the C–H bond in methane and hydrocarbon products. The HBr oxidation takes place on the catalyst surface and bromination of methane should take place only in the gas-phase to avoid the oxidation of methane. Different oxide and phosphate catalysts were studied for methane oxybromination. It was found that HBr oxidation catalysts (CeO_2, TiO_2, RuO_2) produce, beside brominated products and CO, a significant amount of undesired CO_2, which cannot be utilized in later processes and needs to be separated. Basic oxygen sites and high mobility of surface oxygen are the reason for the strong oxidizing character of these catalysts which leads to the oxidation of carbon species. Therefore, phosphate catalysts with moderate oxidizing character were studied for this reaction [49]. $FePO_4$ was shown previously to be very effective [52]. Several iron phosphate catalysts were also prepared by Wang et al. [53,54]. They found that the redox capacity of iron phosphates was responsible for bromine radical generation on the catalyst surface. All catalysts showed considerable activity at 640 °C. Oxidative bromination on the $FePO_4/SiO_2$ catalyst yielded a 50% methane conversion and a total selectivity of 96% for CH_3Br + CO at 570 °C in [52]. A redox route based on the results of comparison experiments and associated characterization was proposed. Among phosphate catalysts [49] vanadium phosphate (VPO) was the best catalyst, with a high selectivity for methyl bromide and a low selectivity for CO_2. The yield of CH_3Br achieved at 480 °C was around 16% and the conversion of CH_4 around 20%. One gram of catalyst was used with a total flow of 100 mL/min consisting of 4.5 vol% CH_4, 1.5 vol% O_2, 3 vol% HBr, and 3 vol% Ar with He balance. The catalyst exhibited excellent HBr oxidation activity but low activity for combustion of methane and products with oxygen. This was confirmed experimentally where the performance of the VPO for each separate reaction of combustion and HBr oxidation were compared. The results suggested that the activation barrier for C–H bond cleavage is rather high and that bromination takes place in the gas phase [49].

In another study [50], lanthanum vanadate catalysts were prepared, tested, and thoroughly characterized. Vanadium oxide introduced redox properties to the material which are absent in pure La_2O_3. This is a consequence of V^{5+}/V^{4+} redox couple and oxygen vacancies. Six catalysts with different V/La molar ratios were prepared with the general formula $LaV_xO_{2.5x+1.5}$ with x being 0, 0.2, 0.5, 0.7, 1, and 1.2 (Figure 2). The catalysts were evaluated in a packed bed reactor at 500 °C and 100 mL/(g min) of gas flow with a composition of CH_4:HBr:O_2:Ar:He = 6:6:3:4.5:80.5. In the case of pure La_2O_3, catalyst particles agglomerated and the gas flow was blocked within 1 h on stream. With other catalysts significant differences in stability were observed. The catalyst with x = 1.2 deactivated to

lower than 50% of its initial activity within 20 h. The most active and stable catalyst was $LaV_{0.5}O_{2.75}$ which did not deactivate for 60 h. The conversion of methane was around 25%, the selectivity to methyl bromide was around 66%, and there was 24% selectivity for dibromomethane, the rest was CO_x. It was shown that a higher yield can be achieved if the empty zone after the catalyst bed is larger, which promotes the gas phase reaction between methane and bromine and thus decreases bromine yield for 0.1 g of catalyst. This again confirms the generation of Br_2 by HBr oxidation and bromination in the gas phase. The catalysts with $x < 0.2$ and catalysts with $x > 1$ were not active. Their loss of activity was shown to be a consequence of LaOBr particle sticking in the former, and to the volatilization of free V_2O_5 in the latter catalyst [50].

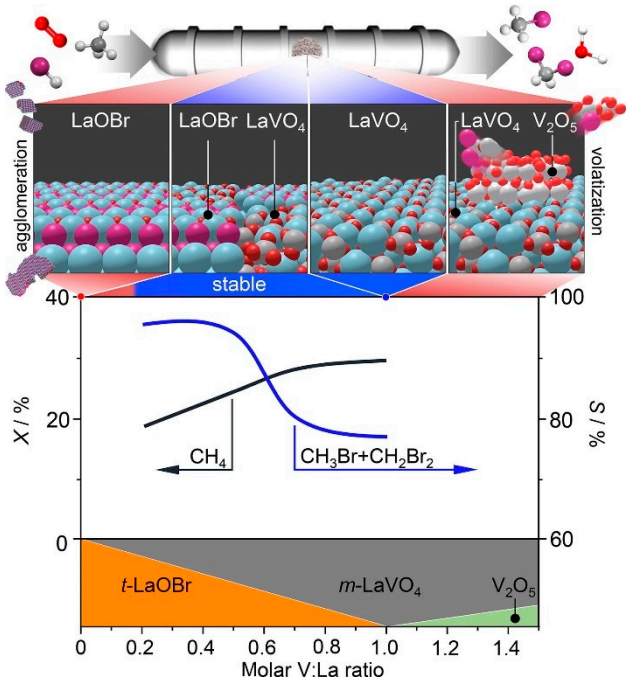

Figure 2. Structure–performance relationships of $LaV_xO_{2.5x+1.5}$ catalysts in methane oxybromination as a function of the molar V:La ratio. Obtained with permission from [50].

Noble metals (Pd, Rh, Ir, Ru, Pt) supported on SiO_2 also showed a good potential for methane oxybromination and oxychlorination [51]. The nominal metal loading of the prepared catalysts was 1 wt%. The highest selectivity for halogenated products was obtained over Pd/SiO_2 for both reactions. At 10% conversion of methane in the oxychlorination reaction, the selectivity for chlorinated products was 95% and the selectivity for brominated products of 98.5% was achieved at 20% conversion in the oxybromination reaction at 480 °C and at 6000 mL/(g h) hourly space velocity with feed composition ratios CH_4:HX:O_2:Ar:He of 6:6:3:4.5:80.5, where HX is either HBr or HCl. The catalyst was stable for more than 40 h on stream. The activity was established as follows: $Ru/SiO_2 > Pt/SiO_2 > Ir/SiO_2 > Rh/SiO_2 \approx Pd/SiO_2$ in methane oxychlorination and $Ru/SiO_2 \approx Ir/SiO_2 \approx Pd/SiO_2 > Pt/SiO_2 > Rh/SiO_2$ in methane oxybromination. It was found that the selectivity to bromomethanes was higher (92–98.5%) than to chloromethanes (78–83%) at moderate CH_4 conversion (20%), but the trends in the product distribution were identical. Ir/SiO_2, Rh/SiO_2, and Pd/SiO_2 were revealed as the most selective catalysts with their ability to reduce and form metal halides. In addition, it was shown that catalytic activity depends on the halide type. During CH_4 oxyhalogenation, an important role of gas-phase halogenation was established based on kinetic studies coupled with operando photoelectron photoion coincidence spectroscopy (PEPICO) for the detection of radicals. At a larger loading of Pd (2 wt% and 5 wt%) there was practically no difference in the activity of the methane oxychlorination reaction; however, by increasing Pd loading, the activity of the catalyst and its selectivity towards brominated products

was decreased, and the selectivity for carbon oxides was increased. XRD patterns of the spent catalyst with 2 and 5 wt% of Pd used in the oxychlorination reaction showed peaks for Pd and PdO consistent with the catalyst with 1 wt% of Pd. When the Pd catalysts that were used for the oxybromination reaction were analyzed, the differences in XRD diffractograms of materials with a higher Pd loading were observed compared to the 1 wt% Pd/SiO_2 catalyst. At higher loading the metallic reflection appeared which was not observed on the spent catalyst with a lower loading of Pd. Raman and XPS (X-ray photoelectron spectroscopy) analysis also showed that the oxide phase was also present on the catalyst with 5 wt% of Pd. The intensity of Br 3d peak in XPS spectrum was lower in the 5 wt% Pd/SiO_2 catalyst compared to the 1 wt% Pd/SiO_2 catalyst. Therefore, the decreased activity and selectivity was attributed to these changes. The catalyst had a stronger oxidic character when the loading was higher, which promoted the formation of CO_x and decreased the selectivity towards brominated products. The mechanism of the oxyhalogenation reactions over Pd/SiO_2 catalyst was also thoroughly investigated and the presence of methyl radicals in the gas phase during both of the reactions was confirmed by operando photoelectron photoion coincidence (PEPICO) spectroscopy. Also Br radicals were detected during the oxybromination of methane, while Cl radicals were detected when the reactants were O_2 and HCl only. It was concluded that the gas phase reactions in the oxybromination of methane have a greater contribution to the overall activity than in the oxychlorination of methane over 1 wt% Pd/SiO_2 catalyst. In the latter case it was estimated that at least half of the methane conversion rate can be attributed to the gas phase reactions. However, the formation of C–X (where X is Br or Cl) on the catalyst active sites was not undoubtedly excluded [51].

For the Rh/SiO_2 catalyst, methyl bromide was successfully produced from methane, oxygen, and hydrogen bromide [55]. The active bromine species were $Br^{\bullet}$ radicals and Br surface species, which were formed by HBr oxidation. HBr also inhibited deep oxidation and methane steam reforming, which provided a high selectivity for CH_3Br. The reaction occurs both in the gas phase and on the catalyst surface. In another work [56], Rh/SiO_2 catalyst was further investigated and either CH_3Br or CH_3Br and CO were produced. After 650 h on stream it still showed excellent catalyst stability. It was found that for CH_3Br production, the catalyst calcination temperature should be 900 °C. $FePO_4/SiO_2$ catalyst was also studied [57]. Good catalyst stability and a high selectivity towards CH_3Br showed after 200 h on stream; however at longer time periods coke deposition became problematic. A maximum methane conversion of 50% was achieved. Wang et al. [58] produced acetic acid from methane over the Ru/SiO_2 catalyst. HBr was recycled and almost 100% CH_3Br conversion was achieved in a two-step process. Silica-supported oxide catalysts were also tested for the same reaction [59]. It was found that deep oxidation is prevented by using catalysts which lack facile redox ability, such as BaO/SiO_2. Methane conversion of 44% with 95% selectivity for CH_3Br, CH_3OH, and CO was achieved, but the catalytic performance degraded after 30 h. Wang et al. [60] also studied the effect of SiO_2, MgO, and Al_2O_3 supports on the methane oxybromination over Rh, Ru, Pd, and Pt-based catalysts. Rh/SiO_2 showed the highest activity with 20% CH_4 conversion and 70% of CH_3Br selectivity. The influence of catalyst-type support on the catalytic activity and product distribution in the reaction of methane oxybromination was determined.

Zichittella et al. [61] compared oxychlorination and oxybromination of methane over RuO_2, Cu-K-La-X, CeO_2, VPO, TiO_2, and $FePO_4$ catalysts. It was established that the product distribution is dependent of the type of halogen and the catalyst behavior. The authors found the relationships among the oxyhalogneation, gas-phase halogenation, and hydrogen halide and methane oxidation. Oxyhalogenation activity of the catalysts followed RuO_2 > Cu-K-La-X > CeO_2 > VPO > TiO_2 > $FePO_4$, and was correlated with their ability to oxidize the hydrogen halide and the gas-phase reactivity of the halogen with methane. The highest catalytic activity with the HX feedstock was achieved for the CeO_2 catalyst with selectivities and yields of chloromethanes (>82% and 28%) and bromomethanes (>98% and 20%), respectively. The catalyst characterization results can be seen in Figure 3.

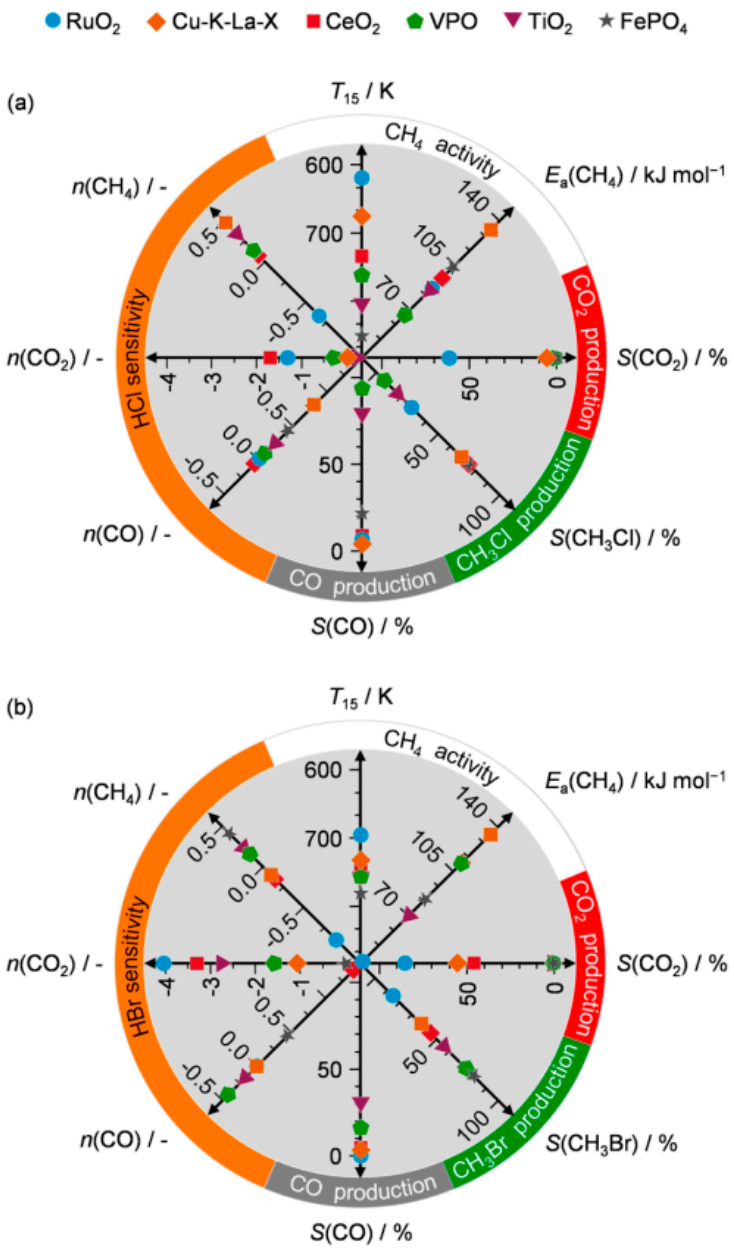

Figure 3. Overview of the catalytic descriptors in (**a**) methane oxychlorination and (**b**) methane oxybromination. The upper half of the radar charts classifies a material as a good oxyhalogenation catalyst if it combines high activity and low propensity to CO_2 formation. The bottom half classifies materials for their ability to produce CH_3X. Reprinted from [61].

Pieters et al. [62–64] studied oxyhydrochlorination of methane (CH_4 + 1x HCl + 0.5x O_2 → $CH_{4-x}Cl_x$ + xH_2O) on fumed silica supported catalysts prepared by impregnation with CuCl, KCl, and $LaCl_3$. About 70% yield of chloromethane was achieved for catalysts containing 41.7 wt% of CuCl, 11.5 wt% KCl, and 9.4 wt% $LaCl_3$. The temperature was 245 °C and the feed composition O_2:CH_4:HCl was 32:19:49 with a residence time around 2.8 s. The effect of the support in KCl and $CuCl_2$ catalysts for oxychlorination of methane were investigated by Garcia et al. [65] a few years later. The compared supports were SiO_2 and γ-Al_2O_3. It was found that strong interaction of copper ions with Al_2O_3 support was present but it was absent in the SiO_2 supported Cu catalyst. Alumina stabilized Cu^{2+} ions. The catalytic activity was improved by the addition of K in catalysts with high K/Cu ratio. This was attributed to the lowering of the melting point of metal chloride mixtures on the catalysts which were molten during the reaction. Thus chlorine activity was increased due to the higher rate of chlorine

evolution. This was especially evident on Al_2O_3 supported catalysts. When additional $LaCl_3$ was introduced to K–Cu catalyst the activity was improved even more. Garcia and Resasco further studied the role of $LaCl_3$ in catalysts for the oxychlorination of methane [66]. The improved stability and activity in La promoted $CuCl_2$–KCl catalysts supported on γ-Al_2O_3 and SiO_2 stems from the inhibiting role of La on K–Cu segregation on the catalyst. Without La, segregation of K–Cu was observed on SiO_2 by XRD, differential thermal analysis, SEM, and electron paramagnetic resonance.

Peringer et al. [67,68] synthesized and tested $LaCl_3$ catalysts for oxidative methane chlorination. $LaCl_3$ is a highly stable and selective catalyst for this reaction. A hypochlorite transient species acts as the active site on the surface. $LaCl_3$ allows for modifying the activity and selectivity of the reaction by catalyst modification, as opposed to the radical gas phase chemistry of copper catalysts. The oxidative chlorination of methane using lanthanum (LaOCl and $LaCl_3$) catalysts with Co, Ni, and Ce added was further studied by Peringer et al. [69] in another work. The authors found that Co and Ce metal dopants lead to a higher conversion of methane due to strong redox active sites and the enhanced oxygen adsorption capacity, which might be related to a higher concentration of OCl^- active sites. Earlier, the same group with Podkolzin et al. [70] showed that LaOCl and $LaCl_3$ catalysts are active and stable in methyl chloride production even after 3 weeks of testing. The authors established that the presence of oxygen is important for catalytic activity and methane activation proceeds on the surface of the catalyst based on the conducted kinetic measurements. The lanthanum-based catalysts exhibited 100% selectivity towards CH_3Cl at CH_4 conversion below 1–2 mol%. When the methane conversion increased, CH_3Cl was the main product, but at the same time CH_2Cl_2, CO, and CO_2 byproducts appeared.

Amorphous and mesoporous ZrO_2 catalyst were also tested [71]. ZrO_2 is a non-redox catalyst which showed higher activity and stability in methane oxychlorination than conventional ZrO_2. Stable operation was achieved for 50 h at 470 °C without significant deactivation. A methane conversion of 18.6% was achieved.

4. Multi-Step Processes

As the products of methane halogenation reactions are often highly reactive molecules, it should come to no surprise that they are often immediately converted to further chemicals in the same process. In the so-called multi-step processes, the products of the halogenation reaction are merely intermediates for the formation of the final product. Most often, these sorts of processes involve some active metal which can couple the intermediates, for example by providing oxygen, while being halogenated itself, and is then de-halogenated to produce the halogen, and thus the catalytic cycle is completed. The targeted products of such processes cover a broad range, including alcohols, ethers and light olefins. In this section, examples of such processes are covered and the underlying chemistry is illuminated.

A typical example of a multi-step halogenation process is the conversion of ethane to different products via the bromination reaction [72]. In the study, ethane was first brominated to ethyl bromide, which was then transformed in a subsequent step to different products, as can be seen in Figure 4. For this transformation, different metal oxides were used, which lead to the generation of different products. The three metal oxide mixtures used in the study were a 50/50 CuO/ZrO_2 mixture (MO-1), a 43/7/50 mixture of $Co_3O_4/Sm_2O_3/ZrO_2$ (MO-2), and a 50/50 mixture of Co_3O_4/ZrO_2 (MO-3). MO-1 and MO-2 were used at temperatures of 200 °C to 250 °C to produce primarily ethanol and diethyl ether, while MO-3 was used at 350 °C, producing mainly ethylene. The authors also tested the metal oxides for methane conversion in the same type of process, where the product selectivities (based on converted bromoalkanes) were 52% to methanol and 38% to CO_2 for MO-1. For MO-2, significantly more promising results were attained with a methanol selectivity of 44%, dimethyl ether selectivity of 44%, and CO_2 selectivity of 11%.

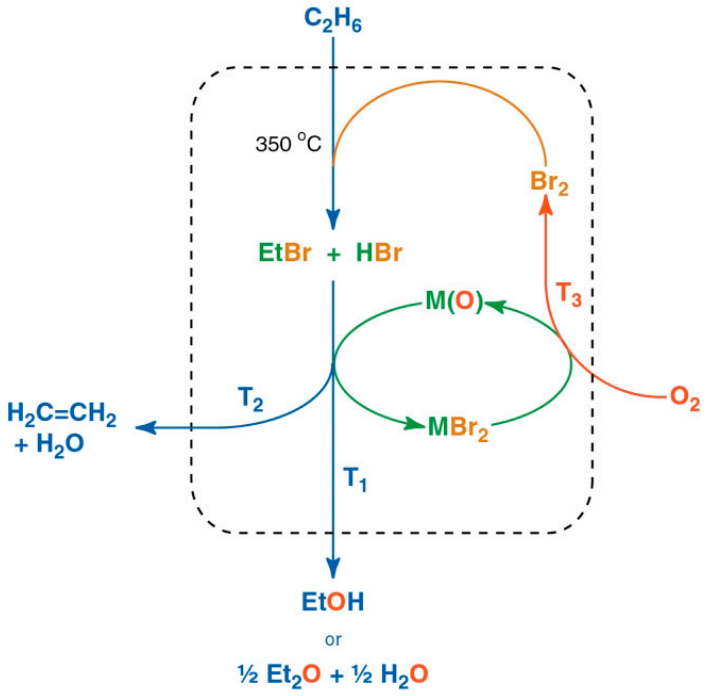

Figure 4. An example of a multi-step process involving halogenation—generation of ethanol or diethyl-ether from ethane. Reproduced from [72] with permission from the Centre National de la Recherche Scientifique (CNRS) and The Royal Society of Chemistry.

A significant amount of work in this field was performed by the group of Ford [73–75]. In one of the studies, methane coupling was performed by a two-step process started with methane bromination, which was followed by condensation using a CaO/zeolite composite catalytic material, producing C1–5 hydrocarbons and aromatics with high selectivity [73]. In a follow-up study, the authors presented an investigation of a broader range of conditions, including different temperatures [74]. The resulting selectivities to different hydrocarbons are presented in Figure 5. In the study, the authors also proposed a cyclic reactor operated by feeding solely methane and oxygen, while all the bromine is recycled internally. In another work, the authors studied a similar process as mentioned above—an integrated process for transforming methane or ethane to alcohols, ethers or olefins via bromination and condensation over metal oxides. A wide array of combinations of metal (Fe, Co, and Cu) oxides, supported on different materials (SiO_2, TiO_2, ZrO_2) was covered in the study, which had a significant effect on the selectivity. Notably, in ethane coupling, Co favored diethyl ether formation while ethanol was the major product in cases of Fe. Cu results were highly dependent on metal oxide formulation, producing methanol, acetone, and CO_2 in some cases and methanol and diethyl ether in others [75].

Targeted dimethyl ether synthesis from methane via bromination was covered by the group of Zhou in two studies [76,77]. The process consisted of two steps—first, methane bromination to bromomethane was carried out over a 0.1 wt% Ru/SiO_2 catalyst. Afterwards, dimethyl ether synthesis from CH_3Br was carried out over $RuCl_3$ catalyst [77].

The authors tested both of the reaction steps under different conditions and achieved relatively high selectivities and conversions, as presented in Table 1. The authors also noted a potential drawback of the process related to the corrosive nature of HBr at elevated temperatures. In order to better elucidate the catalytic activity and stability, the authors synthesized and tested a wide array of different catalysts (MCl_{2-3}/SiO_2, M being Zn, Mg, Co, Mn, Ni, Cu, and Fe) in a follow-up study [76]. They identified 12 mol% $ZnCl_2/SiO_2$ catalyst to be the most active in the second step CH_3Br hydrolysis to DME (dimethyl ether). They also performed a thorough stability study of the catalyst, performing the reaction at different temperatures and flow rates and testing various $ZnCl_2$ loadings. The authors concluded that the catalyst, while being highly active, inevitably deactivates over time due to the loss

of Cl^- anions. The catalyst was successfully regenerated to some degree, but was not able to reach the levels of activity of a fresh catalyst.

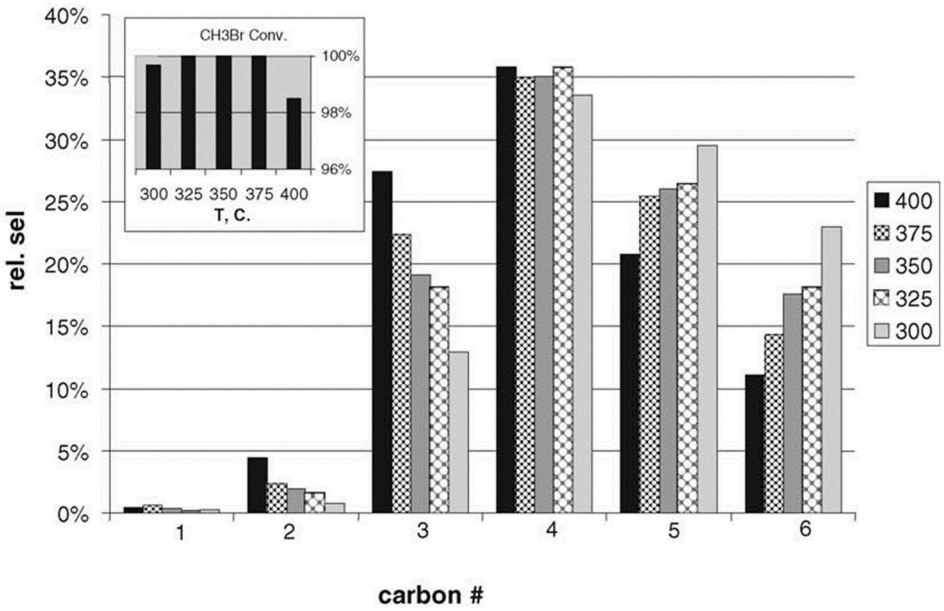

Figure 5. Products of methane bromination and coupling over Ca/ZSM-5 at different temperatures. Carbon numbers 1–4 are predominantly olefins (with trace amounts of alkanes), while 5 and 6 are a mixture of alkanes and alkenes. Reproduced with permission from [74].

Table 1. Conversions and selectivities of both stages of the DME (dimethyl ether) synthesis via bromination. Reproduced with permission from [77].

Methane oxidative bromination results using the Ru/SiO_2 catalyst						
T (°C)	**CH_4 (mL/min)**	**O_2 (mL/min)**	**CH_4 conversion (%)**	**Selectivity (%)**		
				CH_3Br	**CH_2Br_2**	**CO**
530	5	15	27.6	80	1.9	18.2
530	5	20	24.4	89.4	1.7	8.8
560	5	20	31.8	78.8	2.3	18.9
Methanol and DME synthesis over $RuCl_3$ catalyst						
T (°C)	**H_2O (g)**	**CH_3Br (g)**	**CH_3Br conversion (%)**	**Selectivity (%)**		
				DME	**CH_3OH**	
150	0.7	0.5	66.1	22.2	77.8	
170	0.7	0.5	83.2	55	45	
180	0.7	0.5	97	58.7	41.3	
180	0.4	0.5	60.5	43.7	56.2	
180	0.6	0.5	87	62.7	37.3	
180	0.7	0.5	71.8	48.7	51.3	
180	0.7	0.5	98.3	68.9	31	

In another bromination-based study by Wang et al. [78], acetic acid was produced in a two-step process of methane oxidative bromination and carbonylation/hydrolysis. In the study, the authors first concluded a screening study of different multi-functional catalytic materials for the oxidative bromination of methane, identifying the 2.5% Ba, 2.5% La, 0.5% Ni, 0.1% Ru/SiO_2 catalyst as the most appropriate, achieving 62.9% single-pass methane conversion with CH_3Br, CH_2Br_2, CO, and CO_2 selectivities of, respectively, 54.5%, 5.3%, 34.6%, and 5.6% at 600 °C. The conversion achieved surpassed 70% after increasing the reaction temperature over 660 °C; however, there was a drastic decrease in

CH_3Br selectivity and an increase in CO selectivity. In the subsequent step of acetic acid synthesis, the authors tested an $RhCl_3$ catalyst with different amounts of KI and PPh_3 as promotors. The latter increased the reaction rate, and a final 97.7% yield of acetyl bromide was achieved.

While the aforementioned processes were related mainly to bromination, methane/ethane chlorination as the first step is another possible scenario. In an earlier study, Marquaire et al. [79] investigated the possibility of homogenous gas-phase reaction as the second step. In their case, the reagents used were CH_3Cl and Cl_2, and the authors deemed the process "chloro-pyrolysis". The process takes place at high temperatures (600–970 °C) and atmospheric pressure, with short (40 ms) residence times. With 5% Cl_2 at 950 °C, they achieved 14% CH_3Cl conversion and over 65% selectivity towards C_{2+} products, the majority of them being C_2H_3Cl (32%), C_2H_2 (18%), C_2H_4 (9%), and C_4H_4 (6%). The unwanted side products were CH_4 (15%) and CH_2Cl_2 (20%). At lower temperatures (<900 °C), the CH_2Cl_2 selectivity was higher than 50% (~100% at 600 °C), indicating that the process should be carried out at high temperatures. Furthermore, the authors clarified the advantages of chlorine addition since it increases the reaction rate, lowers soot formation, and increases the formation of C_2H_3Cl.

In another chlorination study, Shalygin et al. [80] synthesized a novel $K_4Ru_2OCl_{10}/TiO_2$ catalyst for the methane/ethane chlorination step. They compared it to a RuO_2/TiO_2 catalyst, and the former showed higher selectivities to methyl- (80%) and ethyl- (90%) chlorides, achieving conversions in the range of 15–20% with the main side products being CO_2 and CO. At temperatures higher than 250 °C, when ethane was used, a high selectivity to ethylene (30%) was observed already in the chlorination step. Furthermore, in-situ FTIR (Fourier-transform infrared spectroscopy) was used to determine that the key intermediate for ethyl chloride and ethylene formation is an ethoxy species, and a methoxy group in the case of methane. For the second step, different catalysts were tested, and especially the 0.02% Pt-SO_4/Zr-Si catalyst showed excellent performance and stability for the synthesis of ethylene and propylene with approximately 100% combined selectivity at 25% conversion.

Osterwalder and Stark [81] investigated the conversion of methyl bromide by the reaction with $AlBr_3$ in an autoclave reactor at 210 °C. The products were light hydrocarbons and the reaction could be efficiently incorporated in the process of methane valorization through bromination. It was stated that in the overall process up to 77% of methane could be converted to hydrocarbons. Additionally, the carbon deposits that were formed during MeBr conversion can be converted to small hydrocarbons (including methane), that are in the same range as obtained by conversion of MeBr, by hydrogen regeneration.

A two-step process of converting methane to liquid hydrocarbons through chlorinated methane products was also proposed [82]. Gasoline range products were obtained by first converting methane to chloromethane over silica supported CuCl-KCl-$LaCl_3$ catalyst prepared according to reports by Pieters [62]. At 330 °C a range of products was obtained at different 3 different GHSV used and 330 °C, mainly CH_3Cl (59.6–85.1%), and CH_2Cl_2 (27–10.7%). The feed stream had a composition of CH_4:HCl:O_2 = 2:2:1. The conversion of methane was 42.7% at the lowest GHSV and 18.4% at the highest GHSV. The conversion of pure methyl chloride to liquid hydrocarbons was achieved using the HZSM-5 catalyst at 350 °C. Most liquid products that were obtained consisted of 10 or less carbon atoms and aromatics. No detailed analysis of liquid products was provided. It was noted that also 2-chloropropane and 2-chloropropane were present in the liquid mixture [82]. It can be observed from these studies that a multi-step conversion of ethane or methane to useful chemicals such as acids, alcohols, ethers, and olefins is feasible and can be highly efficient. In many of the studies reviewed, a possibility of closed-cycle operation is envisioned, enabling the need to only feed methane/ethane and oxygen into the system, making the process promising as a means to convert light alkanes. The most commonly identified potential weaknesses were catalyst stability and halogen intermediate corrosion; however, these can be tackled with smart reactor and catalyst design.

5. Density Functional Theory (DFT)

Yin et al. [83] theoretically studied the mechanism of methane decomposition on ceria and a possible chaperon effect of HCl. Using the DFT+U (DFT with a semiempirically tuned numerical

parameter method) approach due to the *f* electrons of Ce, they modeled the reaction on CeO_2(111), CeO_2(111) with oxygen vacancies, and CeO_2(110). They found out that HCl preferentially adsorbs dissociatively on CeO_2(111) with the adsorption energy 1.1 eV so that H binds to the exposed oxygen atom and Cl attaches to the Ce atom. The adsorption of HCl in the molecular form is ~0.6 eV less favorable. On CeO_2(110), the dissociative adsorption mode is similar but stronger (E_{ads} = 1.7 eV). The calculated energy profiles can be seen in Figure 6.

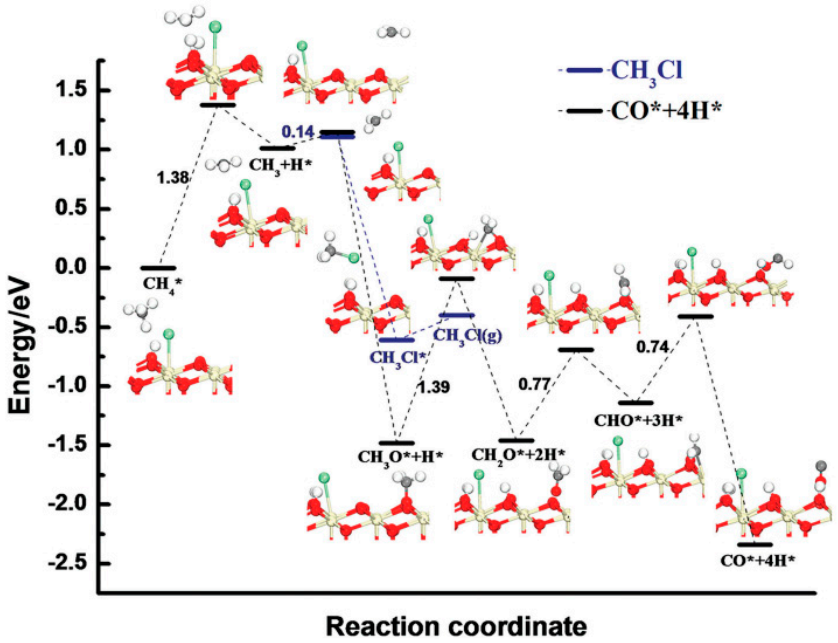

Figure 6. Calculated energy profiles and structures of the key states of CH_4 oxidation at CeO_2(111) with co-adsorbed HCl. Reprinted with permission from [83].

However, the presence of pre-adsorbed dissociated HCl does not help with methane activation. The barriers for hydrogen stripping are virtually unchanged by the presence of HCl. In all instances of CeO_2(111), the first two dehydrogenations (to CH_3 and CH_2) are more difficult (E_A = 1.4 eV) than the last two (yielding CH and CO) with barriers of ~0.7 eV. Instead, HCl opens up a new reaction route. Once CH_3 is formed, it equally readily binds with the adsorbed Cl to form CH_3Cl or with the surface O to form CH_3O. Further chlorination of CH_3Cl was not studied. On the surface with an oxygen vacancy, the CH_3Cl pathway is less likely than full oxidation (via CH_3O), which is also slower. The reduced surface has a higher electron density, which the dehydrogenation of methane further increases. Repulsive interactions between the localized electrons then come into play. CeO_2(110) is a more reactive surface and was found to exhibit better selectivity for oxychlorination to CH_3Cl and higher activity, which the authors attribute to its flatness. The barrier of the first dehydrogenation is 0.3 eV lower than on CeO_2(111).

Litvinenko and Rudakov [84] studied the activation of methane in the gaseous phase with HOCl with and without a spectator water molecule. They found out that these reactions require a preactivation of HOCl, which occurs by a spin transition between the singlet and triplet state. The minimum energy crossing point (MECP) of the two states of HOCl is 34.4 kcal/mol above the singlet state. With the reactants in the triplet state, a lower-lying transition state is accessible, which is typical of two-state reactivity (TSR). Thus, the reaction proceeds through a triplet transition state. CH_3, Cl, and H_2O are formed in a direct reaction between CH_4 and HOCl with a Gibbs activation barrier of 14.2 kcal/mol relative to the triplet pre-reaction state. With H_2O participating, the reaction follows a similar mechanism and energetics, yielding CH_3, two H_2O, and Cl. In both cases, CH_3 and Cl readily recombine. A singlet mechanism, where CH_3Cl and H_2O form in a concerted fashion through a ring-like transition state, is ~20 kcal/mol higher in energy.

Direct chlorination of methane is plagued by deep chlorination reactions, yielding CH_2Cl_2, $CHCl_3$, and CCl_4. It is advantageous to add SO_2 to the process, thereby forming methanesulfonyl chloride (MSC). This compound can be thought of as a CH_3Cl reservoir because it decomposes into SO_2 and CH_3Cl. Kang et al. [85] reported on experimental and theoretical studies of MSC decomposition. They studied the reaction in the gaseous phase. They showed that SO_2Cl^- is a good leaving group after MSC is attacked by a nucleophile, which is Cl^-, $Al_2Cl_7^-$, or 1-methylimidazolium chloride in their study. The energy barriers for their attacks are 11.8, 50.0, and 24.7 kcal/mol, respectively. All reactions proceed through the concerted S_{N2} mechanism.

Paunović et al. [86] investigated bromination of methane experimentally and theoretically, comparing the oxybromination route over vanadyl pyrophosphate (VPO) and europium oxybromide (EuOBr) catalysts and the non-catalyzed bromination with Br_2 in the gaseous phase. They limited the theoretical calculations to the energetics of the intermediates and found that O_2 adsorbs dissociatively on VPO in an exothermic reaction (−0.36 eV/oxygen atom). Upon dissociative adsorption of HBr, Br and OH are formed in a strongly exothermic step (−0.9 eV). It is possible for the Br radical to desorb (barrier of 1.30 eV). If a second molecule of HBr adsorbs dissociatively, Br_2 and H_2O are formed and desorbed with barriers of 0.6 and 1.3 eV, respectively. In the gaseous phase, an equilibrium between Br and Br_2 exist. Bromine radical can abstract a hydrogen from CH_4 (barrier of 0.73 eV). The formed CH_3 reacts with Br_2 to form CH_3Br, while HBr is re-adsorbed on the surface for the regeneration of Br and Br_2. The authors showed that Br* appears at lower temperatures than CH_3*, proving that its generation must be surface-catalyzed as opposed to homogeneous dissociation of Br_2. The activation of CH_4 by adsorbed oxygen (O*) or adsorbed bromine atoms (Br*) is energetically less favored. This catalyst was also tested in reference [49], where a high selectivity for methyl bromide was determined as well as excellent HBr oxidation activity. It was found that bromination occurs in the gas phase. The described mechanism on EuOBr was found to be analogous.

Podkolzin et al. [70] showed that lanthanum-based catalysts ($LaCl_3$ and LaOCl) effectively catalyze chlorination of methane with O_2 and HCl. While O_2 is necessary for the reaction, HCl is not. Without HCl, the reaction starts using up chlorine from the catalyst, effectively transforming $LaCl_3$ into LaOCl. As this transformation is reversible, $LaCl_3$ can function as a chlorine reservoir. With DFT, they showed that O_2 binds dissociatively to the surface, forming the OCl species. This species reacts with gaseous CH_4, yielding CH_3Cl and OH. Peringer et al. [67] found that the hypochlorite transient species acts as the active site on the surface. The catalyst is regenerated when an HCl molecule reacts with OH, yielding gaseous H_2O and surface Cl. Experimentally, however, they did not detect the OCl species and thus labeled it transient. A selectivity of 100% towards CH_3Cl was obtained under 2% conversion, and at higher conversions, CH_2Cl_2, CO, and CO_2 were also formed.

Chistyakov et al. [87] studied the potential energy surface for the reaction between CH_4 and CBr_3^+ with and without assistant nucleophiles ($AlBr_4^-$, $AlCl_4^-$, $Al_2Cl_7^-$) at the B3LYB and PBE level. Generally, these reactions involve a hydride transfer. Without the assistant nucleophile, CH_4 and CBr_3^+ preliminarily form a weakly bound adduct. Traversing a cyclic transition state, an activated product $CH_3BrCBr_2H^+$ is formed. In the presence of assistant nucleophiles, an analogous transition state yields CBr_3 or CCl_3 and $CH_3BrAlBr_3$ or CH_3ClAlC_3 or $CH_3Al_2Cl_7$.

6. Green Processes and Fuel

In addition to being valuable feedstock for the manufacture of bulk chemicals in the chemical industry sector, natural gas, with methane as its main constituent, is also important in the energy sector as it contains chemically bound energy. A considerable part of known exploitable natural gas resources is located in remote regions, far from potential consumers. Transportation of natural gas over long distances is a highly complex operation as it requires high pressure pipelines and means of boosting its pressure by compressors. Also, being in gaseous state, it consumes a much greater amount of energy for its transportation than a comparable amount of liquid fuels would. Conversion of methane into

value-added chemicals and fuels has therefore been a "holy grail" in industry and academia for many years [88]. In this section, a part of the efforts to achieve it is presented.

Gas-to-liquid technologies that have been brought to the commercial scale in the past several decades are mainly based on Fischer–Tropsch [89]. The Fischer–Tropsch process converts synthesis gas (mixture of CO, CO_2, and H_2) into higher hydrocarbons. An autothermal and/or steam reforming step is required for the production of synthesis gas from natural gas [89], which enormously increases the complexity of the technology and its capital investment requirements, making it unsuitable for small and distant natural gas sources. Reforming reactions are done in a fixed bed catalytic reactor at around 20 bar and 1000 °C [89]. High temperatures are required because of the highly endothermic nature of reactions between methane and steam. In steam reformers, heat is provided indirectly through the walls of reformer tubes, while in autothermal reformers a part of the feed reacts with oxygen in an exothermic way, thus providing heat for the endothermic steam methane reforming. The methanol to gasoline process, pioneered by Mobile, used a zeolite based catalyst (H-ZSM-5) for the conversion of methanol to higher hydrocarbons [89,90]. Commercial conversion of methanol took place in an adiabatic fixed bed reactor at 350–410 °C and 20 bar, with a part of the product recycled for temperature control of the highly exothermic reaction [90]. Fluidized bed reactors have also been considered with advantages of easy temperature control and coked catalyst regeneration [90]. In a similar way as methanol is coupled to gasoline components on H-ZSM-5 or to olefins on SAPO-34, methyl halides can also be used as precursors for higher hydrocarbons [18,90]. Methyl halides can be obtained from methane and elemental halogen in one step by either free radical homogeneous or heterogeneous catalytic reactions [30,91]. Compared to the methanol-to-gasoline route, methyl halide routes do not require the complex synthesis gas production step and methanol production step, making this route more attractive especially for smaller production scales. The methyl halide route to higher hydrocarbons is composed of methyl halide synthesis (21), methyl halide coupling (22), and hydrogen halide regeneration (23):

$$CH_4 + nX_2 \rightarrow CH_{4-n}X_n + nHX \quad (21)$$

$$mCH_3X \rightarrow (CH_2)_m + mHX \quad (22)$$

$$2HX + O_2 \rightarrow X_2 + H_2O \quad (23)$$

where X represents the halogen element. All reactions (21)–(23), except those with iodine as halogen, are exothermic [30].

Reaction (21) was studied, for example, by Lombard et al. [92] in a chlorine/methane system in the temperature range between 600 and 1000 °C in an annular plug flow reactor, made of quartz, at atmospheric pressure and 10–30 ms residence time. Although a continuously stirred reactor (CSTR) would be preferred for kinetics studies, as it has no space and time gradients, a tubular reactor was most probably chosen for its simplicity. The reaction was homogenous free radical halogenation. They compared their experimental results to simulations by literature kinetics, which included reacting 99 species and 504 (in majority) irreversible elemental reactions, and obtained a good agreement from which they concluded that the applied reaction mechanism of chloro-pyrolysis was valid. They found out that the increase of chlorine to methane ratio leads to an increase of methylene chloride yield. Poly-substituted methane compounds (e.g., CH_2Cl_2) are undesired in the coupling step (22), so they suggested use of a stepwise introduction of chlorine in the reaction mixture to obtain a higher methyl chloride selectivity.

Methane, with more than one hydrogen substituted with a halogen element, is a major cause of coking and subsequent coupling catalyst deactivation [17,93]. It therefore has to be eliminated from the reaction mixture prior to the coupling reactions, and if this is done by distillation, it can have a significantly negative impact on the process economy [93]. Ding et al. [17] suggest converting dibromomethane (DBM) into either higher hydrocarbons or methyl bromide using hydrogen. They studied the reaction using a silica supported catalyst and discovered that Pd_6C/SiO_2 is effective in the transformation of DBM into higher hydrocarbons (HCs), while Ru/SiO_2 is effective in the

transformation to methyl bromide. The reported selectivity and conversion were 25% (higher HCs) and 85% for Pd_6C/SiO_2 and 87% (CH_3Br) and ~17% for Ru/SiO_2. The reaction conditions were 350 °C, residence time was 2 s, and the DBM:H_2:N_2 mole ratio was 7:14:40. They used a packed bed reactor at atmospheric pressure and considered the temperature range from 200–400 °C. The use of packed bed reactors for catalyst testing is of course a reasonable choice due to its simplicity. As they, however, observed some coke formation on their catalysts, other types of reactors or reactor configurations could be considered as well; e.g., the fluidized bed reactor, as those, used in fluid catalytic cracking (FCC), are especially suited for continuous catalyst regeneration. On the other hand, if catalyst coking is slow, parallel fixed bed reactors in "revolver type" operation could also be considered. In this arrangement, one reactor is in operation, while others are in the regeneration phase. Ding et al. [17] suggest using propane, a side product of methyl bromide to liquids technology, as a feedstock for hydrogen production with steam reforming. With the aim of developing a gas-to-liquids technology, not based on complex reforming, this would however seem to be counterproductive. Ding et al. [93] also proposed the conversion of DBM into methyl bromide using iodine as the homogenous catalyst:

$$CH_2Br_2 + CH_4 \rightarrow 2CH_3Br \quad (24)$$

They performed reaction experiments in a tubular reactor, made of a glass tube, at atmospheric pressure in range of 400–525 °C. According to their results [93], methyl bromide selectivity would be considerably improved with increasing temperature in this temperature range, even approaching equilibrium values. Homogenous catalysis however suffers from a major drawback that is the need for its separation from the reaction mixture using economically expensive thermo-diffusion operations. Additionally both approaches [17,93] are questionable from the thermodynamic point of view. It is unknown if DBM would react into less substituted methyl bromide, if it is present, only if a catalyst is added. In equilibrium one can expect polysubstituted methane to exist. In the case of a homogenous system [93], where no additional reactant was added, one could hardly expect that the system, closer to equilibrium, would move away from the equilibrium conditions by adding a catalyst. If the equilibrium mixture is assumed to come from bromination, the catalyst cannot change it. On the contrary, a methane–DBM mixture can be converted into some methyl bromide if none is initially present. Ding et al. [93] used only methane-pure DBM mixture (without methyl bromide) at the reactor inlet with no methyl bromide.

Hydrogen halide regeneration into halogen is necessary for economic, environmental, and safety reasons. It was studied by Upham et al. [18] using chemical looping of a molten salt. They considered 68 different metal bromides/oxide systems and chose the KBr-LiBr-$NiBr_2$ eutectic system. The selection was made based on thermodynamics and practical criteria such as cost, reactivity, and boiling points. The following reactions took place in due course of their study:

$$NiBr_2 + \frac{1}{2}O_2 \rightarrow NiO + Br_2 \quad (25)$$

$$2HBr + NiO \rightarrow NiBr_2 + H_2O \quad (26)$$

NiO is a suspension of solid particles in a LiBr-KBr system while $NiBr_2$ is soluble in LiBr-KBr [18]. This feature is especially attractive, since mechanical attrition of particles cause problems with the increase of the surface area or with filtering. As NiO was consumed, the solid phase disappeared and was reformed in the regeneration step (Equation (25)). Upham et al. [18] also considered using a molten phase on a SiO_2 solid carrier in a packed-bed and found that this option was not the best because of the lower overall activity in HBr capture. Considerable cracking of propylene, the model compound for higher HCs, and associated coking were also observed when they used SiO_2 supported $NiO/NiBr_2$. The probable cause for less coking and cracking of HCs in the molten phase, as compared to a SiO_2 supported system, was suggested to be the considerably lower solubility of HCs in the molten salt, as opposed to the solubility of HBr [18]. Hydrogen bromide capture and regeneration of bromine

took place at approximately the same temperature ranges as methane activation with bromination and downstream coupling (385–530 °C), making the proposed Br_2 regeneration very suitable for integration into the entire gas to liquid process [18]. They argue that by applying a $NiBr_2$-KBr-LiBr molten salt system for the process with a production of 500 000 t/a of HCs, they could considerably reduce the required process equipment (compressors, heat exchangers, separators, and reactors) for highly corrosive process media and associated capital investment [18]. They estimated that the total heat exchanger duty exposed to a corrosive environment could be reduced from 581 MW (conventional process) to 205 MW (proposed process). The process diagram of the system, relying on the proposed method of HBr capture and bromine regeneration, and the process diagram of the system relying on the conventional approach are shown in Figure 7 [18]. The proposed system could utilize the bubble column slurry reactor for HBr capture and $NiBr_2$ regeneration. Both reactors would operate at around 500 °C. The transfer of molten phase between reactors could be achieved with mechanical (e.g., centrifugal pumps), made of corrosion resistant materials, or even more conveniently using the "airlift" effect of process gas in the HBr capture reactor and air/oxygen in the regeneration reactor. In the latter case, no contact of equipment between the moving parts and the corrosive media would be made.

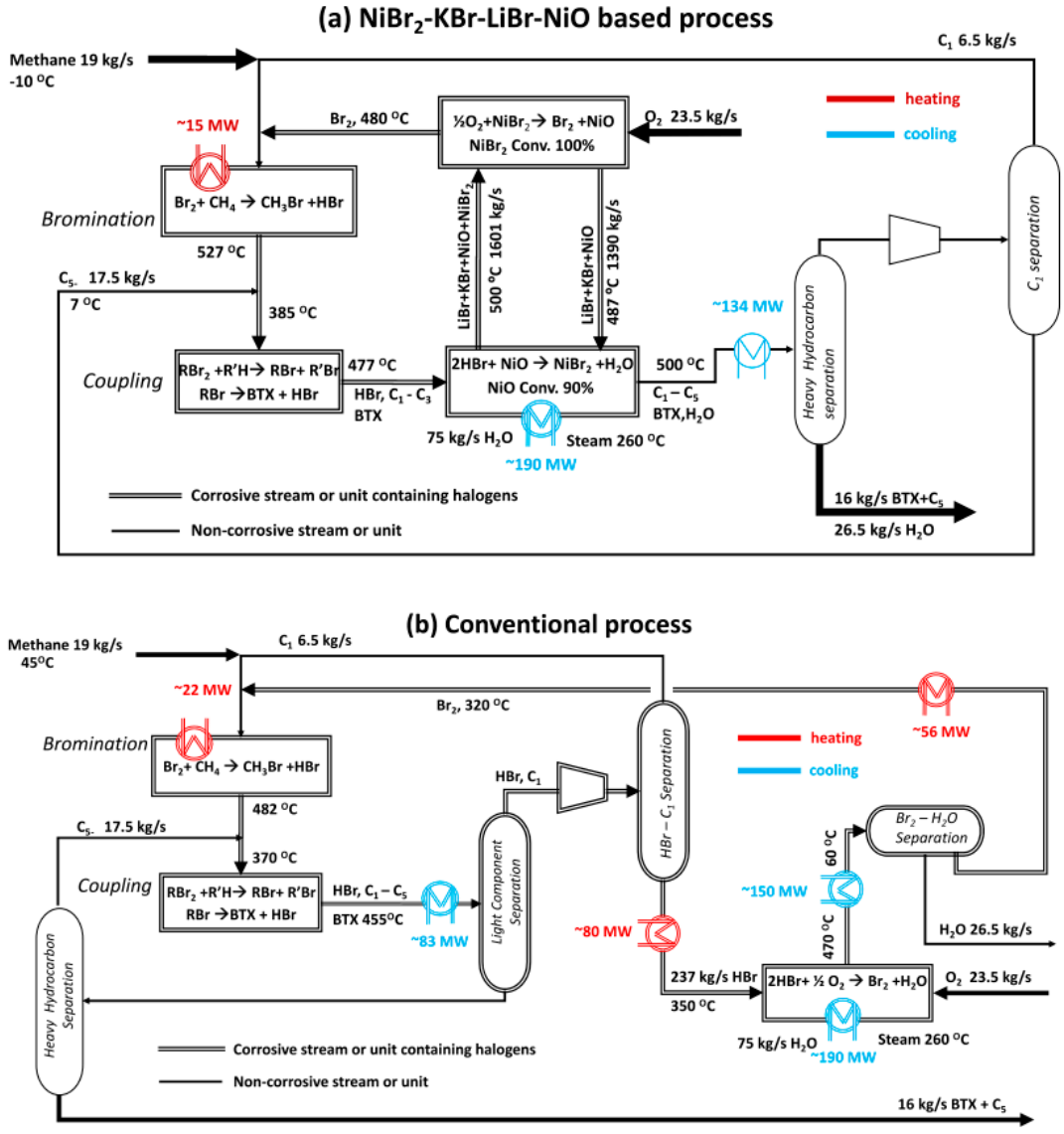

Figure 7. The proposed and conventional process for the conversion of methane to higher hydrocarbons [18].

Besides the production of fuels or chemicals, which is the goal of the gas-to-liquid technologies, a greener energy production from methane using a bromination–oxidation cycle was considered by Rebordinos et al. [94]. They argue that the capture and storage of carbon dioxide obtained by methane combustion to prevent its emissions to atmosphere would require up to 40% energy released by methane conversion. They suggested a conversion of methane to coke using bromine, with coke being more easily separated from the gaseous mixture, and not presenting any long term disposal problem compared to carbon dioxide [94]:

$$CH_4 + 2Br_2 \rightarrow C(s) + 4HBr \quad (27)$$

$$4HBr + O_2 \rightarrow 2Br_2 + 2H_2O \quad (28)$$

$$CH_4 + O_2 \rightarrow C(s) + 2H_2O \quad (29)$$

where reaction (29) is a summary reaction of the entire process, schematically shown in Figure 8. All reactions are exothermic. Figure 9 presents the flowsheet of the bench-scale plant for methane bromination.

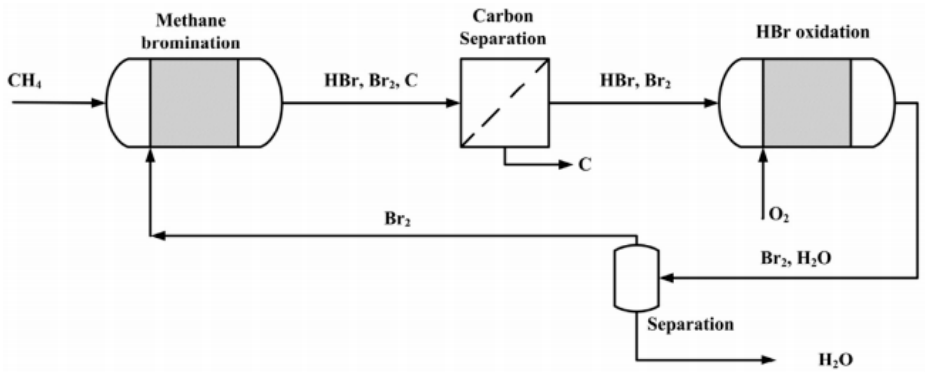

Figure 8. Schematic representation of methane oxidation in bromine mediated processes for energy and coke production. Reprinted from [94].

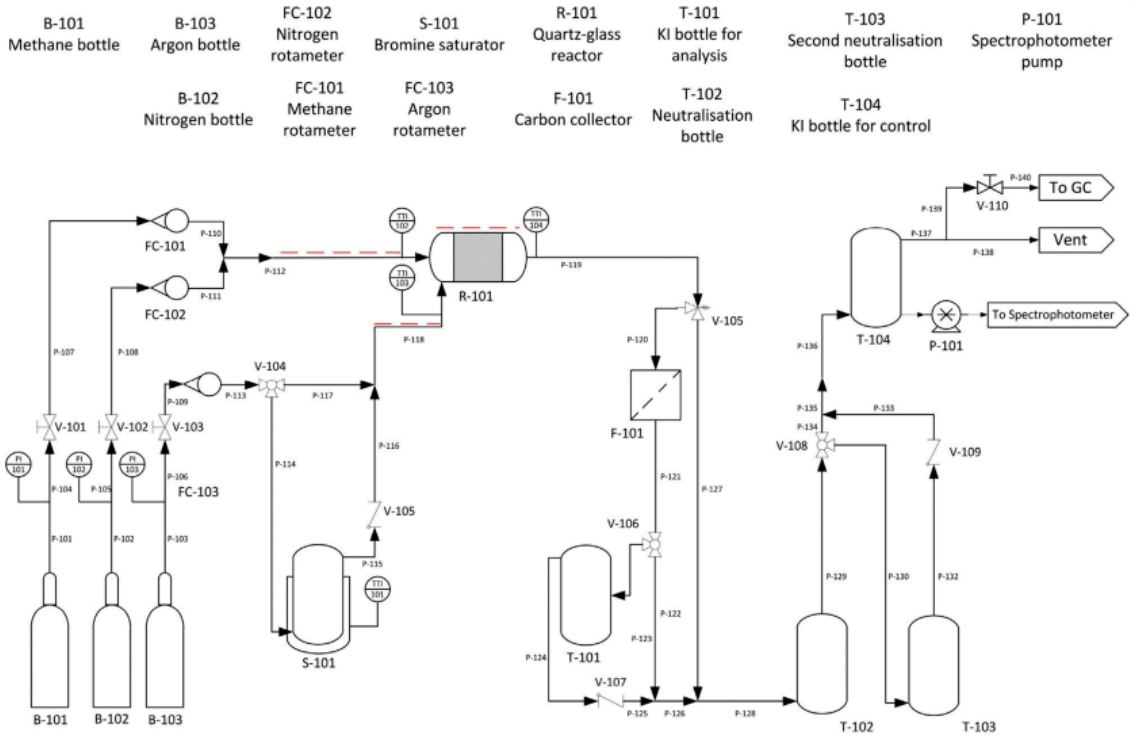

Figure 9. Flowsheet of the bench-scale plant for methane bromination. Reprinted from [94].

As no carbon dioxide is formed, only about half of the chemical energy, stored in methane, can be liberated that way, which is compensated for by the amount of energy that would be needed for carbon capture and storage (CCS) [94]. The proposed process was studied experimentally in a quartz glass reactor at atmospheric pressure and at temperatures of about 1000 °C, and also theoretically [94]. Although one of the reactors used had a quite high diameter to length ratio, the tubular reactor would be the closest approximation. They report that although carbon formation starts at 500 °C, it becomes noticeable only at temperatures beyond 750 °C [94]. The amount of bromine bound to coke was dependent on the reaction temperature: the higher the temperature, the lesser the amount of bromine [94]. A simulation with the SANDIA mechanism at 600 °C suggested that coke formation was the limiting step of the entire process and not the reactions between methane and bromine [94]. Coke was deposited on the reactor surface and filtered. In the future they intend to apply strategies for the prevention of the fouling of the reactor walls and to eliminate residual traces of bromine in the coke produced [94]. Perhaps both challenges could be elegantly solved by applying a fluidized bed coking process, such as, for example, fluid coking and flexicoking from the petroleum industry [95]. In this case coke would be preferentially deposited on the fluidized coke particles, which would also provide scraping action on the reactor walls, preventing excessive coke buildup.

Amongst halogens used for the activation of methane, bromine seems to be best choice, because HBr can be more easily regenerated compared to HCl or HF [93,94] and is more reactive than iodine [94]. The halogenation approach to methane activation is attractive from another point of view. The reactions involved (methane halogenation, coupling, and halogen regeneration) are in general exothermic. This means that in principle no additional energy is required for a process to operate. The reaction heat can be recovered and used as a utility for heating, driving process machinery, or electrical power production.

7. Unconventional Technologies

In addition to thermochemical halogenation of methane, unconventional methods of methane activation are also being widely researched. They include the application of ultrasound, plasma, superacids, and light.

Van Iersel et al. [96] applied ultrasound in controlled methyl chloride synthesis. They relied on extreme temperature and pressure pulses encountered during the formation and collapse of cavitation bubbles at 293 K to increase the selectivity of the methane–chlorine reaction towards methyl chloride. Highly diluted (0.22%) chlorine in methane was used. Since no methylene chloride was observed they concluded that the reaction was very selective. Although high pressures are no challenge for the modern chemical industry, they claim that their process is inherently safe because it takes place at atmospheric pressure and can be stopped immediately when the ultrasound source is turned off.

A pulsed discharge plasma method was applied by Okumoto et al. [97]. Although they were mainly focused on the reaction between methane and oxygen to obtain oxygenates, they did some experiments on the reaction between methane and iodine. Iodine was simply put in solid form on the reactor wall, which raises the question if the results were qualitative because of the lack of any control over such a type of reactant introduction. They claim the reaction was selective towards CH_3I (95% selectivity) and that no polyiodine products could be observed, with only traces of ethane detected [97].

Batamack et al. [98] studied classical thermochemical chlorination of methane over superacidic catalysts. They increased the poor selectivity of free radical homogenous reactions by the use of SO_4^{2-}/ZrO_2 catalyst at temperatures below 240 °C. At the gas hourly space velocity of 1 L/(g h), a methane to chlorine ratio of 4:1, and 200 °C, they obtained 30% chlorine conversion and 90% selectivity towards methyl chloride. When the temperature was increased to 235 °C, the selectivity dropped to 80%. The reduction of selectivity with the increase of temperature was attributed to the increased contribution of non-selective free radical homogenous reactions on the total yield and selectivity [98]. In addition, they added Fe, Pt, and Mn to SO_4^{2-}/ZrO_2 base material. They found

out that these elements increased the selectivity of the catalyst but at the penalty of reduced activity. 1.5%Fe/0.5%Mn/4% SO_4^{2-}/ZrO_2 catalyst was not active at 200 °C, but it provided 90% selectivity and 40% conversion at 235 °C.

Vilenchich et al. [99] applied a gamma source for the initiation of the reaction between methane and iodine in the gas phase between 80 and 230 °C using a batch reactor. According to their research, the temperature had a smaller effect on the process compared to the introduction of energy by gamma radiation. Optimal methyl iodide yield (60%) was obtained at 130 °C, 7 mol% of I_2 in the mixture, 8×10^{14} eV/g, and at a dose of 1230 rad. They claim that the cost of gamma energy is insignificant to the cost of chemicals, but arguments in support of this claim were not presented.

Methane chlorination reaction yield and selectivity in a flow-through tubular photo-reactor under the influence of UV light was studied by Cabrera et al. [100]. Although in their case methylene chloride was the desired product, almost 75% selectivity towards methyl chloride was obtained at low (~10%) methane conversion. They also tried to describe their results using kinetics obtained from literature and obtained good results when they fitted kinetic parameters to their experimental data by allowing them to change at most 5% from the initial literature values.

Liebov et al. [101] studied photo-oxygenation of light alkanes using iodine oxides and chloride. Their desired product was methyl-trifluoroacetic acid (Me-TFA), so only rough conclusions can be drawn on the selectivity towards methyl chloride, which in their case was the undesired product. They used a batch reactor, where they introduced 100 psi of CH_4 with KCl and NH_4IO_3 dissolved in trifluoroacetic acid. Methyl chloride was presumably obtained from the methyl radical and the chlorine atom from KCl; its yield was increased when KCl concentration was increased. Selectivity towards Me-TFA was increased by increasing methane pressure, therefore for methyl chloride the opposite should hold. Visible light was worse for selectivity towards Me-TFA and with the same reasoning as before should be better for higher methyl chloride selectivity. Nevertheless, reaction times were long (24 h) and selectivities towards methyl chloride were low (the highest methyl chloride yield was approximately 5%) and it can be concluded that this type of methane activation would not be suitable for large scale industrial application.

Chlorination of methane was shown to be achievable also through a mechanochemical gas–solid reaction. Methane at 0.5–1.5 vol.% in N_2 was flown through a milling vial filled with a solid catalyst, trichloroisocyanuric acid (TCCA) (source of chlorine), and milling balls. The reaction was initiated and carried out at 10 Hz shaking frequency and at 112.5 °C. The most effective tested catalyst was ceria. The selectivity to methyl chloride was almost 100% and the maximum chlorine transferred from TCCA was 30%. The process is interesting because it can be carried out under low temperatures and non-corrosive conditions [102].

It can be concluded that the unconventional technologies described cannot compete with more classical thermochemical routes. Amongst the literature studied in the scope of this work, an exception can be given to the application of superacids. All other processes need additional energy to operate [96,97,99–101] as opposed to the thermochemical way where at least on larger scales the reaction heat could be recovered for useful purposes (e.g., steam and electricity generation). It is also questionable if the claimed improved selectivity towards mono-halogenated methane and benign reaction conditions outweigh the disadvantages of increased energy consumption, system complexity, and reactor size. It has to be taken into account that the benign reaction conditions in terms of low pressure and temperature also demand larger equipment since the reactions at those conditions are much slower than at high pressures and temperatures. The application of benign conditions, e.g., almost room temperature, also eliminates any possibility of efficient heat recovery.

8. Conclusions

Since Olah's investigation of methane halogenation, the reaction has become more relevant due to the increased availability of natural gas and its relatively low price. Gas phase halogenation and its mechanisms and kinetics were already extensively studied in the past. Kinetics of methane bromination

were studied in 1944 [21] and kinetics of methane chlorination with elementary steps were studied in 1997 [33]. The focus of ongoing research today is therefore aimed at the development of catalysts for the halogenation and oxyhalogenation of methane, and at the investigation of mechanisms on these new catalysts, in order to increase the selectivity to the desired halogenated product. Methane bromination is usually preferred since the C–Br bond is weaker than C–Cl bond, and it offers an easier way for subsequent reactions of halogen elimination. Zeolites have proven to be somewhat efficient in improving methyl halide yield; however, it is questionable if the zeolites act as catalysts with their active sites, or if their system of pores merely serves as the confinement for the reactants. Therefore, the mechanism of action is not entirely understood. Most promising catalysts for oxybromination are based on vanadium phosphate. Here the reactions, similarly as in the case of catalytic halogenation, take place both in the gas phase and on the catalyst surface, where the catalyst serves mainly for the oxidation of HBr. With the development of density functional theory methods and with the increasing computational power available, it has become possible to investigate the mechanisms of methane halogenations theoretically; however the number of studies investigating the mechanism of methane halogenation, especially on catalysts, is relatively low.

The process of the production of chloromethanes via gas phase chlorination of methane is almost a century old; it was developed by Hoechst in 1923 and is still in use today [103]. Catalytic processes of methane halogenation are not yet commercialized, but with the integration of halogenation, hydrogen halide regeneration, and conversion of halogenated products to more useful and less corrosive products, this kind of process could be suitable for use directly on the natural gas production sites. Although several unconventional reactors and processes were proposed, the use of conventional reactors for catalytic halogenation of methane, hydrogen halide regeneration, and further conversion of halogenated products is most likely the most convenient way to achieve the economic feasibility.

Supplementary Materials: The following are available online at http://www.mdpi.com/2227-9717/8/4/443/s1, Table S1: List of chemical species appearing in methane thermochlorination kinetic scheme from ref. [14,15], Table S2: Microkinetic model of methane halogenation using iodine and bromine in the gas phase from ref [17].

Author Contributions: Conceptualization, D.B. and A.P.; writing—original draft preparation, D.B., M.G. (Matic Grom), D.L.J., A.K., M.H., M.G. (Miha Grilc), A.P.; writing—review and editing, D.B., A.P. and M.G. (Miha Grilc); supervision, B.L. All authors have read and agreed to the published version of the manuscript.

Funding: The authors acknowledge the financial support from the Slovenian Research Agency (research core funding No. P2–0152 and project J2-1724).

Acknowledgments: The authors also gratefully acknowledge Vili Resnik for his warm support.

Conflicts of Interest: The authors declare no conflict of interest.

References

1. Anderson, R.B.; Kölbel, H.; Rálek, M. *The Fischer-Tropsch Synthesis*; Academic Press: Waltham, MA, USA, 1984; Volume 16.
2. Ma, Y.; Ge, Q.; Li, W.; Xu, H. Methanol synthesis from sulfur-containing syngas over Pd/CeO_2 catalyst. *Appl. Catal. B Environ.* **2009**, *90*, 99–104. [CrossRef]
3. Song, C. Global challenges and strategies for control, conversion and utilization of CO_2 for sustainable development involving energy, catalysis, adsorption and chemical processing. *Catal. Today* **2006**, *115*, 2–32. [CrossRef]
4. Tian, P.; Wei, Y.; Ye, M.; Liu, Z. Methanol to olefins (MTO): From fundamentals to commercialization. *ACS Catal.* **2015**, *5*, 1922–1938. [CrossRef]
5. Bjørgen, M.; Joensen, F.; Holm, M.S.; Olsbye, U.; Lillerud, K.-P.; Svelle, S. Methanol to gasoline over zeolite H-ZSM-5: Improved catalyst performance by treatment with NaOH. *Appl. Catal. A Gen.* **2008**, *345*, 43–50. [CrossRef]
6. Zaidi, H.A.; Pant, K.K. Catalytic conversion of methanol to gasoline range hydrocarbons. *Catal. Today* **2004**, *96*, 155–160. [CrossRef]

7. Conte, M.; Lopez-Sanchez, J.A.; Zhou, W.; Morgan, D.J.; Ryabenkova, Y.; Bartley, J.K.; Carley, A.F.; Taylor, S.H.; Kiely, C.J.; Khalid, K.; et al. Modified zeolite ZSM-5 for the methanol to aromatics reaction. *Catal. Sci. Technol.* **2012**, *2*, 105–112. [CrossRef]
8. Schwach, P.; Pan, X.; Bao, X. Direct Conversion of Methane to Value-Added Chemicals over Heterogeneous Catalysts: Challenges and Prospects. *Chem. Rev.* **2017**, *117*, 8497–8520. [CrossRef]
9. Galadima, A.; Muraza, O. Revisiting the oxidative coupling of methane to ethylene in the golden period of shale gas: A review. *J. Ind. Eng. Chem.* **2016**, *37*, 1–13. [CrossRef]
10. Sun, K.; Ginosar, D.M.; He, T.; Zhang, Y.; Fan, M.; Chen, R. Progress in Nonoxidative Dehydroaromatization of Methane in the Last 6 Years. *Ind. Eng. Chem. Res.* **2018**, *57*, 1768–1789. [CrossRef]
11. Xie, P.; Pu, T.; Nie, A.; Hwang, S.; Purdy, S.C.; Yu, W.; Su, D.; Miller, J.T.; Wang, C. Nanoceria-Supported Single-Atom Platinum Catalysts for Direct Methane Conversion. *ACS Catal.* **2018**, *8*, 4044–4048. [CrossRef]
12. Guo, X.; Fang, G.; Li, G.; Ma, H.; Fan, H.; Yu, L.; Ma, C.; Wu, X.; Deng, D.; Wei, M.; et al. Direct, nonoxidative conversion of methane to ethylene, aromatics, and hydrogen. *Science* **2014**, *344*, 616–619. [CrossRef] [PubMed]
13. Taifan, W.; Baltrusaitis, J. CH_4 conversion to value added products: Potential, limitations and extensions of a single step heterogeneous catalysis. *Appl. Catal. B Environ.* **2016**, 525–547. [CrossRef]
14. Wei, y.; Zhang, D.; Liu, Z.; Su, B.-L. Methyl halide to olefins and gasoline over zeolites and SAPO catalysts: A new route of MTO and MTG. *Chin. J. Catal.* **2012**, *33*, 11–21. [CrossRef]
15. Zhang, A.; Sun, S.; Komon, Z.J.A.; Osterwalder, N.; Gadewar, S.; Stoimenov, P.; Auerbach, D.J.; Stucky, G.D.; McFarland, E.W. Improved light olefin yield from methyl bromide coupling over modified SAPO-34 molecular sieves. *Phys. Chem. Chem. Phys.* **2011**, *13*, 2550–2555. [CrossRef]
16. Zhang, D.; Wei, Y.; Xu, L.; Chang, F.; Liu, Z.; Menga, S.; Su, B.-L.; Liu, Z. MgAPSO-34 molecular sieves with various Mg stoichiometries: Synthesis, characterization and catalytic behavior in the direct transformation of chloromethane into light olefins. *Microporous Mesoporous Mater.* **2008**, *116*, 684–692. [CrossRef]
17. Ding, K.; Derk, A.R.; Zhang, A.; Hu, Z.; Stoimenov, P.; Stucky, G.D.; Metiu, H.; McFarland, E.W. Hydrodebromination and Oligomerization of Dibromomethane. *ACS Catal.* **2012**, *2*, 479–486. [CrossRef]
18. Upham, D.C.; Snodgrass, Z.R.; Tabatabaei, M.; McConnaughy, T.B.; Gordon, M.J.; Metiu, H.; McFarland, E.W. Molten salt chemical looping for reactive separation of HBr in a halogen- based natural gas conversion process. *Chem. Eng. Sci.* **2017**, *160*, 245–253. [CrossRef]
19. Pérez-Ramírez, J.; Mondelli, C.; Schmidt, T.; Schlüter, O.F.-K.; Wolf, A.; Mleczko, L.; Dreier, T. Sustainable chlorine recycling via catalysed HCl oxidation: From fundamentals to implementation. *Energy Environ. Sci.* **2011**, *4*, 4786–4799. [CrossRef]
20. Horn, R.; Schlögl, R. Methane Activation by Heterogeneous Catalysis. *Catal. Lett.* **2015**, *145*, 23–39. [CrossRef]
21. Kistiakowsky, G.B.; Van Artsdalen, E.R. Bromination of Hydrocarbons. I. Photochemical and Thermal Bromination of Methane and Methyl Bromine. Carbon-Hydrogen Bond Strength in Methane. *J. Chem. Phys.* **1944**, *12*, 469–478. [CrossRef]
22. Lorkovic, I.M.; Sun, S.; Gadewar, S.; Breed, A.; Macala, G.S.; Sardar, A.; Cross, S.E.; Sherman, J.H.; Stucky, G.D.; Ford, P.C. Alkane bromination revisited: "reproportionation" in gas-phase methane bromination leads to higher selectivity for CH3Br at moderate temperatures. *J. Phys. Chem. A* **2006**, *110*, 8695–8700. [CrossRef] [PubMed]
23. McBee, E.T.; Hass, H.B.; Neher, C.M.; Strickland, H. Chlorination of methane. *Ind. Eng. Chem.* **1942**, *34*, 296–300. [CrossRef]
24. Golden, D.M.; Walsh, R.; Benson, S.W. The Thermochemistry of the Gas Phase Equilibrium $I_2 + CH_4 \leftrightarrow CH_3I + HI$ and the Heat of Formation of the Methyl Radical1. *J. Am. Chem. Soc.* **1965**, *87*, 4053–4057. [CrossRef]
25. Pease, R.N.; Walz, G.F. Kinetics of the thermal chlorination of methane. *J. Am. Chem. Soc.* **1931**, *53*, 3728–3737. [CrossRef]
26. Rashid, H.U.R.; Yu, K.; Zhou, J. Advances in the Development of Methane Bromination. *J. Chem. Soc. Pak.* **2011**, *33*, 922–928.
27. Aglulin, A.G.; Bakshi, Y.M. Kinetic studies of the mechanism of direct chlorination of methane in the presence of porous fillers. *Kinet. Catal.* **1983**, *24*, 80–86.
28. Pritchard, H.O.; Pyke, J.B.; Trotman-Dickenson, A.F. The study of Chlorine Atom Reactions in the Gas Phase. *J. Am. Chem. Soc.* **1955**, *77*, 2629–2633. [CrossRef]
29. Gordon, A.R.; Barnes, C. The Free Energy, Entropy and Heat Capacity of Bromine and of Hydrogen Bromide from Spectroscopic Data. *J. Chem. Phys.* **1933**, *1*, 692–696. [CrossRef]

30. Degirmenci, V.; Uner, D.; Yilmaz, A. Methane to higher hydrocarbons via halogenation. *Catal. Today* **2005**, *106*, 252–255. [CrossRef]
31. Arai, K.K.Z.; Yoshida, T.M.; Shinoda, K. Rate of consumption of chlorine in thermal chlorination of methane. *Kogyo Kagaku Zassi* **1958**, *61*, 1231–1233. [CrossRef]
32. Rozanov, V.N.; Treger, Y.A. Kinetics of the Gas Phase Thermal Chlorination of Methane. *Kinet. Catal.* **2010**, *51*, 661–669. [CrossRef]
33. Tirtowidjo, M. Fundamental Kinetic Modeling of Industrial Reactors. In Proceedings of the AIChE Annual Meeting, Los Angeles, CA, USA, 16–21 November 1997. Paper 78b.
34. Shah, J.J.; Fox, R.O. Computational Fluid Dynamics Simulation of Chemical Reactors: Application of in Situ Adaptive Tabulation to Methane Thermochlorination Chemistry. *Ind. Eng. Chem. Res.* **1999**, *38*, 4200–4212. [CrossRef]
35. Raman, V.; Fox, R.O.; Harvey, A.D.; West, D.H. CFD Analysis of Premixed Methane Chlorination Reactors with Detailed Chemistry. *Ind. Eng. Chem. Res.* **2001**, *40*, 5170–5176. [CrossRef]
36. Upham, D.C.; Kristoffersen, H.H.; Snodgrass, Z.R.; Gordon, M.J.; Metiu, H.; Mcfarland, E.W. Bromine and iodine for selective partial oxidation of propane and methane. *Appl. Catal. A Gen.* **2019**, *580*, 102–110. [CrossRef]
37. Larsen, P.; Ulin, J.; Dahlstrøm, K.; Jensen, M. Synthesis of [11C] iodomethane by iodination of [11C] methane. *Appl. Radiat. Isot.* **1997**, *48*, 153–157. [CrossRef]
38. Olah, G.A.; Gupta, B.; Felberg, J.D.; Ip, W.M.; Husain, A.; Karpeles, R.; Lammertsma, K.; Melhotra, A.K.; Trivedi, N.J. Electrophilic reactions at single bonds. 20. Selective monohalogenation of methane over supported acidic or platinum metal catalysts and hydrolysis of methyl halides over gamma-alumina-supported metal oxide/hydroxide catalysts. A feasible path for the oxidative conversion of methane into methyl alcohol/dimethyl ether. *J. Am. Chem. Soc.* **1985**, *107*, 7097–7105. [CrossRef]
39. Gorin, E.; Fontana, C.M.; Kidder, G.A. Chlorination of Methane with Copper Chloride Melts Rate of Chlorination. *Ind. Eng. Chem.* **1948**, *40*, 2128–2134. [CrossRef]
40. Paunović, V.; Pérez-Ramírez, J. Catalytic halogenation of methane: A dream reaction with practical scope? *Catal. Sci. Technol.* **2019**, *9*, 4515–4530. [CrossRef]
41. Kim, Y.; Kim, J.; Kim, H.W.; Kim, T.-W.; Kim, H.J.; Chang, H.; Park, M.B.; Chae, H.-J. Sulfated Tin Oxide as Highly Selective Catalyst for the Chlorination of Methane to Methyl Chloride. *ACS Catal.* **2019**, *9*, 9398–9410. [CrossRef]
42. Degirmenci, V.; Yilmaz, A.; Uner, D. Selective methane bromination over sulfated zirconia in SBA-15 catalysts. *Catal. Today.* **2009**, *142*, 30–33. [CrossRef]
43. Bucsi, I.; Olah, G.A. Selective monochlorination of methane over solid acid and zeolite catalysts. *Catal. Lett.* **1992**, *16*, 27–38. [CrossRef]
44. Joo, H.; Kim, D.; Lim, K.S.; Choi, Y.N.; Na, K. Selective methane chlorination to methyl chloride by zeolite Y-based catalysts. *Solid State Sci.* **2018**, *77*, 74–80. [CrossRef]
45. Kwon, S.; Chae, H.-J.; Na, K. Control of methane chlorination with molecular chlorine gas using zeolite catalysts: Effects of Si/Al ratio and framework type. *Catal. Today* **2020**. [CrossRef]
46. Paunovic, V.; Mitchell, S.; Verel, R.; Lee, S.S.; Pérez-Ramírez, J. Aluminum Redistribution in ZSM-5 Zeolite upon Interaction with Gaseous Halogens and Hydrogen Halides and Implications in Catalysis. *J. Phys. Chem. C* **2020**, *124*, 722–733. [CrossRef]
47. Batamack, P.T.D.; Mathew, T.; Prakash, G.K.S. One-Pot Conversion of Methane to Light Olefins or Higher Hydrocarbons through H-SAPO-34-Catalyzed in Situ Halogenation. *J. Am. Chem. Soc.* **2017**, *139*, 18078–18083. [CrossRef]
48. Centi, G.; Barbera, K.; Perathoner, S.; Gupta, N.K. Onion-Like Graphene Carbon Nanospheres as Stable Catalysts for Carbon Monoxide and Methane Chlorination. *ChemCatChem* **2015**, *7*, 3036–3046. [CrossRef]
49. Paunović, V.; Zichittella, G.; Moser, M.; Amrute, A.P.; Pérez-Ramírez, J. Catalyst design for natural-gas upgrading through oxybromination chemistry. *Nat. Chem.* **2016**, *8*, 803. [CrossRef]
50. Paunović, V.; Artusi, M.; Verel, R.; Krumeich, F.; Hauert, R.; Pérez-Ramírez, J. Lanthanum vanadate catalysts for selective and stable methane oxybromination. *J. Catal.* **2018**, *363*, 69–80. [CrossRef]
51. Paunović, V.; Zichittella, G.; Hemberger, P.; Bodi, A.; Pérez-Ramírez, J. Selective Methane Functionalization via Oxyhalogenation over Supported Noble Metal Nanoparticles. *ACS Catal.* **2019**, *9*, 1710–1725. [CrossRef]

52. Lin, R.; Ding, Y.; Gong, L.; Dong, W.; Wang, J.; Zhang, T. Efficient and stable silica-supported iron phosphate catalysts for oxidative bromination of methane. *J. Catal.* **2010**, *272*, 65–73. [CrossRef]
53. Wang, R.; Lin, R.; Ding, Y. Model Iron Phosphate Catalysts for the Oxy-bromination of Methane. *Catal. Lett.* **2014**, 1384–1392. [CrossRef]
54. Wang, R.; Lin, R.; Ding, Y.; Liu, J.; Wang, J.; Zhang, T. Structure and phase analysis of one-pot hydrothermally synthesized FePO4-SBA-15 as an extremely stable catalyst for harsh oxy-bromination of methane. *Appl. Catal. A Gen.* **2013**, *453*, 235–243. [CrossRef]
55. Yang, F.; Liu, Z.; Li, W.S.; Zhou, X.P. The Oxidative Bromination of Methane Over Rh/SiO_2 Catalyst. *Catal. Lett.* **2008**, 226–232. [CrossRef]
56. Liu, Z.; Li, W.; Zhou, X. Product oriented oxidative bromination of methane over Rh/SiO_2 catalysts. *J. Nat. Gas Chem.* **2010**, *19*, 522–529. [CrossRef]
57. Lin, R.; Ding, Y.; Gong, L.; Dong, W.; Chen, W.; Lu, Y. Studies on oxy-bromination of methane and coke deposition over FePO4/SiO_2 catalysts. *Catal. Today* **2011**, *164*, 34–39. [CrossRef]
58. Wang, K.X.; Xu, H.F.; Li, W.S.; Zhou, X.P. Acetic acid synthesis from methane by non-synthesis gas process. *J. Mol. Cat. A Chem.* **2005**, *1*, 65–69. [CrossRef]
59. Lin, R.; Ding, Y.; Gong, L.; Li, J.; Chen, W.; Yan, L.; Lu, Y. Oxidative bromination of methane on silica-supported non-noble metal oxide catalysts. *Appl. Catal. A Gen.* **2009**, *353*, 87–92. [CrossRef]
60. Wang, P.; Chen, L.; Shen, S.; Au, C.-T.; Yin, S.-F. Methane oxybromination over Rh-based catalysts: Effect of supports. *Chin. J. Chem. Eng.* **2019**. [CrossRef]
61. Zichittella, G.; Paunovic, V.; Amrute, A.P.; Pe, J. Catalytic Oxychlorination versus Oxybromination for Methane Functionalization. *ACS Catal.* **2017**. [CrossRef]
62. Pieters, W.J.M.; Conner Jr, W.C.; Carlson, E.J. The oxyhydrochlorination of methane on fumed silica-based Cu + 1, K., La catalysts: I. Catalyst synthesis. *Appl. Catal.* **1984**, *11*, 35–48. [CrossRef]
63. Conner Jr, W.C.; Pieters, W.J.M.; Signorelli, A.J. The oxyhydrochlorination of methane on fumed silica-based Cu, K., La catalysts: III. Bulk & surface analysis. *Appl. Catal.* **1984**, *11*, 59–71. [CrossRef]
64. Conner, W.C., Jr.; Pieters, W.J.M.; Gates, W.; Wilkalis, J.E. The oxyhydrochlorination of methane on fumed silica—Based Cu+1, K., La catalysts: II. Gas phase stoichiometry. *Appl. Catal.* **1984**, *11*, 49–58. [CrossRef]
65. Garcia, C.L.; Resasco, D.E. Effects of the support and the addition of a second promoter on potassium chloride-copper (II) chloride catalysts used in the oxychlorination of methane. *Appl. Catal.* **1989**, *46*, 251–267. [CrossRef]
66. Garcia, C.L.; Resasco, D.E. High-temperature oxychlorination catalysts: Role of LaCl3 as an inhibitor of the segregation of active species during heating/cooling cycles. *J. Catal.* **1990**, *122*, 151–165. [CrossRef]
67. Peringer, E.; Tejuja, C.; Salzinger, M.; Lemonidou, A.A.; Lercher, J.A. On the synthesis of LaCl3 catalysts for oxidative chlorination of methane. *Appl. Catal. A Gen.* **2008**, *350*, 178–185. [CrossRef]
68. Peringer, E.; Podkolzin, S.G.; Jones, M.E.; Olindo, R.; Lercher, J.A. LaCl3 -based catalysts for oxidative chlorination of CH_4. *Top. Catal.* **2006**, *38*, 211–220. [CrossRef]
69. Peringer, E.; Salzinger, M.; Hutt, M.; Lemonidou, A.A.; Lercher, J.A. Modified Lanthanum Catalysts for Oxidative Chlorination of Methane. *Top. Catal.* **2009**, 1220–1231. [CrossRef]
70. Podkolzin, S.G.; Stangland, E.E.; Jones, M.E.; Peringer, E.; Lercher, J.A. Methyl Chloride Production from Methane over Lanthanum-Based Catalysts. *J. Am. Chem. Soc.* **2007**, 2569–2576. [CrossRef]
71. Huang, J.; Wang, W.; Li, D.; Xu, S.; Liu, Q.; Chen, X.; Fei, Z.; Zhang, Z. Facile construction of non-crystalline ZrO_2 as an active yet durable catalyst for methane oxychlorination. *J. Sol-Gel Sci. Technol.* **2019**, 163–172. [CrossRef]
72. Zhou, X.; Yilmaz, A.; Yilmaz, G.A.; Lorkovic, I.M.; Laverman, L.E.; Weiss, M.; Sherman, J.H.; McFarland, E.W.; Stucky, G.D.; Ford, P.C. An integrated process for partial oxidation of alkanes. *Chem. Commun.* **2003**, *3*, 2294–2295. [CrossRef] [PubMed]
73. Lorkovic, I.M.; Noy, M.L.; Schenck, W.A.; Weiss, M.; Sherman, J.H.; McFarland, E.W.; Stucky, G.D.; Ford, P.C. C1 coupling via bromine activation and tandem catalytic condensation and neutralization over CaO/zeolite composites. *Chem. Commun.* **2004**, *49*, 566–567. [CrossRef] [PubMed]
74. Lorkovic, I.M.; Noy, M.L.; Schenck, W.A.; Belon, C.; Weiss, M.; Sun, S.; Sherman, J.H.; McFarland, E.W.; Stucky, G.D.; Ford, P.C. C1 oxidative coupling via bromine activation and tandem catalytic condensation and neutralization over CaO/zeolite composites: II. Product distribution variation and full bromine confinement. *Catal. Today* **2004**, *98*, 589–594. [CrossRef]

75. Lorkovic, I.M.; Yilmaz, A.; Yilmaz, G.A.; Zhou, X.; Laverman, L.E.; Sun, S.; Schaefer, D.J.; Weiss, M.; Noy, M.L.; Cutler, C.I.; et al. A novel integrated process for the functionalization of methane and ethane: Bromine as mediator. *Catal. Today* **2004**, *98*, 317–322. [CrossRef]
76. You, Q.; Liu, Z.; Li, W.; Zhou, X. Synthesis of dimethyl ether from methane mediated by HBr. *J. Nat. Gas Chem.* **2009**, *18*, 306–311. [CrossRef]
77. Xu, H.F.; Wang, K.X.; Li, W.S.; Zhou, X.P. Dimethyl ether synthesis from methane by non syngas process. *Catal. Lett.* **2005**, *100*, 53–57. [CrossRef]
78. Wang, K.X.; Xu, H.F.; Li, W.S.; Au, C.T.; Zhou, X.P. The synthesis of acetic acid from methane via oxidative bromination, carbonylation, and hydrolysis. *Appl. Catal. A Gen.* **2006**, *304*, 168–177. [CrossRef]
79. Marquaire, P.-M.; Al Kazzaz, M.; Muller, Y.; Saint Just, J. Methane to vinyl chloride by "Chloro-pyrolysis" of methyl chloride. *Stud. Surf. Sci. Catal.* **1997**, *107*, 269–274. [CrossRef]
80. Shalygin, A.; Paukshtis, E.; Kovalyov, E.; Bal'zhinimaev, B. Light olefins synthesis from C1-C2 paraffins via oxychlorination processes. *Front. Chem. Sci. Eng.* **2013**, *7*, 279–288. [CrossRef]
81. Osterwalder, N.; Stark, W.J. Direct Coupling of Bromine-Mediated Methane Activation and Carbon-Deposit Gasification. *ChemPhysChem* **2007**, *8*, 297–303. [CrossRef]
82. Taylor, C.E.; Noceti, R.P.; Schehl, R.R. Direct conversion of methane to liquid hydrocarbons through chlorocarbon intermediates. *Stud. Surf. Sci. Catal.* **1988**, 483–489. [CrossRef]
83. Yin, L.; Lu, G. A DFT + U study on the oxidative chlorination of CH_4 at ceria: The role of HCl. *Catal. Sci. Technol.* **2017**, 2498–2505. [CrossRef]
84. Litvinenko, S.L.; Rudakov, E.S. DFT analysis of the mechanism for the gas-phase chlorination of methane in the HOCl–H_2O system. *Theor. Exp. Chem.* **2012**, *48*, 212–216. [CrossRef]
85. Zhang, Q. Methanesulfonyl Chloride (CH_3SO_2Cl) Decomposition as a Key Step for Low-Temperature Methane Conversions. *Chem. Eng. Technol.* **2017**, *40*, 656–662. [CrossRef]
86. Paunović, V.; Hemberger, P.; Bodi, A.; López, N.; Pérez-Ramírez, J. Evidence of radical chemistry in catalytic methane oxybromination. *Nat. Catal.* **2018**, *1*, 363–370. [CrossRef]
87. Chistyakov, A.L.; Stankevich, I.V.; Gambaryan, N.P.; Akhrem, I.S. Nucleophilic Assistance in Methane Activation by Superelectrophiles with Halogen-Centered Cationic Sites. *Russ. J. Org. Chem.* **2006**, *42*, 1606–1614. [CrossRef]
88. Al-Douri, A.; Sengupta, D.; El-Halwagi, M.M. Shale gas monetization: A review of downstream processing to chemicals and fuels. *J. Nat. Gas Sci. Eng.* **2017**, *45*, 436–455. [CrossRef]
89. Wood, D.A.; Nwaoha, C.; Towler, B.F. Gas-to-liquids (GTL): A review of an industry offering several routes for monetizing natural gas. *J. Nat. Gas Sci. Eng.* **2012**, *9*, 196–208. [CrossRef]
90. Olsbye, U.; Svelle, S.; Bjørgen, M.; Beato, P.; Janssens, T.V.W.; Joensen, F.; Bordiga, S.; Lillerud, K.P. Conversion of Methanol to Hydrocarbons: How Zeolite Cavity and Pore Size Controls Product Selectivity. *Angewandte* **2012**, *51*, 5810–5831. [CrossRef]
91. Wang, B.; Albarracín-Suazo, S.; Pagán-torres, Y.; Nikolla, E. Advances in methane conversion processes. *Catal. Today* **2017**, *285*, 147–158. [CrossRef]
92. Lombard, C.; Marquaire, P.-M. New study of methane to vinyl chloride process. *Stud. Surf. Sci. Catal.* **2004**, *147*, 529–534. [CrossRef]
93. Ding, K.; Metiu, H.; Stucky, G.D. The Selective High-Yield Conversion of Methane Using Iodine-Catalyzed Methane Bromination. *ACS Catal.* **2013**, *3*, 474–477. [CrossRef]
94. Rebordinos, J.G.; Salten, A.H.J.; Agar, D.W. BrOx cycle: A novel process for CO_2 -free energy production from natural gas. *Int. J. Hydrogen Energy* **2017**, *42*, 4710–4720. [CrossRef]
95. Gary, J.H.; Handwerk, G.E.; Kaiser, M.J.; Geddes, D. *Petroleum Refining—Technology and Economics*, 5th ed.; Taylor & Francis Group: Oxfordshire, UK, 2007. [CrossRef]
96. Van Iersel, M.M.; Van Schilt, M.A.; Benes, N.E.; Keurentjes, J.T.F. Ultrasonics Sonochemistry Controlled methyl chloride synthesis at mild conditions using ultrasound irradiation. *Ultrason. Sonochem.* **2010**, *17*, 315–317. [CrossRef] [PubMed]
97. Okumoto, M.; Mizuno, A. Conversion of methane for higher hydrocarbon fuel synthesis using pulsed discharge plasma method. *Catal. Today* **2001**, *71*, 211–217. [CrossRef]
98. Batamack, P.; Bucsi, I.; Molnar, A.; Olah, G.A. Electrophilic chlorination of methane over superacidic sulfated zirconia. *Catal. Lett.* **1994**, *25*, 11–19. [CrossRef]
99. Vilenchich, R.; Hodgins, J.W. Gamma Initiated Iodination of Methane in the Gas Phase. *Can. J. Chem. Eng.* **1970**, *48*, 588–590. [CrossRef]

100. Cabrera, A.E.C.M.I.; Alfano, O.M. Product yield and selectivity studies in photoreactor design. Theory and experiments for the chlorination of methane. *Chem. Eng. Sci.* **1990**, *45*, 2439–2446. [CrossRef]
101. Liebov, N.S.; Goldberg, J.M.; Boaz, N.C.; Coutard, N. Selective Photo-Oxygenation of Light Alkanes Using Iodine Oxides and Chloride. *ChemCatChem* **2019**, *11*, 5045–5054. [CrossRef]
102. Bilke, M.; Losch, P.; Vozniuk, O.; Bodach, A.; Schuth, F. Methane to Chloromethane by Mechanochemical Activation: A Selective Radical Pathway. *J. Am. Chem. Soc.* **2019**, *141*, 11212–11218. [CrossRef]
103. Rossberg, M.; Wilhelm, P.; Gerhard, P.; Tögel, A.; Theodore, R.T.; Klaus, K.B. *Ullman's Encyclopedia of Industrial Chemistry*; John Wiley & Sons: Hoboken, NJ, USA, 2012; Volume 9, pp. 15–39.